REPORT DOCUMENTATION PAGE

READ INSTRUCTIONS BEFORE COMPLETING FORM

1. REPORT NUMBER: NSWC TR 84-122	2. GOVT ACCESSION NO.
3. RECIPIENT'S CATALOG NUMBER	
4. TITLE (and Subtitle): LOADING AND UTILIZATION OF ACTIVE MATERIAL IN NICKEL COMPOSITE ELECTRODES: OPTIMIZATION	5. TYPE OF REPORT & PERIOD COVERED: '82, '83
	6. PERFORMING ORG. REPORT NUMBER
7. AUTHOR(s): W. W. Lee, W. A. Ferrando, and R. A. Sutula	8. CONTRACT OR GRANT NUMBER(s)
9. PERFORMING ORGANIZATION NAME AND ADDRESS: Naval Surface Weapons Center (Code R32), 10901 New Hampshire Avenue, Silver Spring, MD 20903-5000	10. PROGRAM ELEMENT, PROJECT, TASK AREA & WORK UNIT NUMBERS: 62761N, F61545, SF61-545-601. 3R01AA530, 3R32BH401
11. CONTROLLING OFFICE NAME AND ADDRESS	12. REPORT DATE: December 1984
	13. NUMBER OF PAGES: 57
14. MONITORING AGENCY NAME & ADDRESS (if different from Controlling Office)	15. SECURITY CLASS. (of this report): UNCLASSIFIED
	15a. DECLASSIFICATION/DOWNGRADING SCHEDULE

16. DISTRIBUTION STATEMENT (of this Report)

Approved for public release; distribution unlimited.

17. DISTRIBUTION STATEMENT (of the abstract entered in Block 20, if different from Report)

18. SUPPLEMENTARY NOTES

19. KEY WORDS (Continue on reverse side if necessary and identify by block number)

Composite Plaque
Nickel Electrode
Impregnation
Batteries
Charging Efficiency

20. ABSTRACT (Continue on reverse side if necessary and identify by block number)

Investigations were undertaken to determine the optimum conditions for loading and utilizing nickel hydroxide active material in nickel composite electrodes.

The main emphasis was placed on the improvement of both loading efficiency by electrochemical impregnation and utilization efficiency of the $Ni(OH)_2$ active material. The efficiencies were examined as functions of

20. (Cont.)

such electrochemical conditions as current density, nickel concentration, pH, temperature of the impregnating bath, the continuity of current flow and manner of adding $Co(OH)_2$ additive. Also studied was the loading efficiency of chemical impregnation (polarization method) and the suspension method which enables a direct loading of externally prepared active material into the composite body.

The electrochemical impregnation in a 1.8M Ni^{2+} solution with the application of 80 mA/cm^2 current density achieves over 1.4 $gm/(cm^3$ of electrode volume) loading in two hours. The impregnation time can be substantially reduced (net time less than 30 minutes) in a 3.5M Ni^{2+} solution, however, there exists a danger of active material deposition at the outer surface of plaque. The chemical method achieves a loading efficiency (1.1 $gm/(cm^3$ of electrode volume)) in five impregnation cycles. This is close to the efficiency for a powder sintered body. The great advantage of the composite plaque was manifested by the suspension method which loads over 1.1 $gm/(cm^3$ of electrode volume) of the active material in three very quick impregnation cycles.

The most important factor for a quick utilization of the active material was found to be the additive distribution. Utilization of over 95 percent of active material becomes possible within 2-3 cycles after a brief formation by depositing a thin $Co(OH)_2$ additive film on the surface of the $Ni(OH)_2$ active material.

Finally, a model of the additive distribution in the active material is proposed to account for different patterns of utilization exhibited by the electrodes.

NSWC-TR-84-122

LOADING AND UTILIZATION OF ACTIVE MATERIAL IN NICKEL COMPOSITE ELECTRODES: OPTIMIZATION

BY W. W. LEE W. A. FERRANDO R. A. SUTULA

RESEARCH AND TECHNOLOGY DEPARTMENT

DECEMBER 1984

NAVAL SURFACE WEAPONS CENTER

Dahlgren, Virginia 22448 • Silver Spring, Maryland 20910

FOREWORD

This report explores the optimization of impregnation techniques for NSWC's composite nickel electrode. This study was aimed at achieving not only a quick yet simple method of active material loading, but also fast utilization of the active material.

The results of various impregnation methods, with a special emphasis on electrochemical impregnation are presented and discussed. Various methods of adding the cobalt additive were investigated. The manner of adding the cobalt additive was found to be critically important for achieving a fast rise in utilization as a function of charge-discharge cycles.

A model of the active material distribution in the composite body is presented to account for the diverse behavior of utilization exhibited by the nickel composite electrodes.

Approved by:

JACK R. DIXON, Head
Materials Division

CONTENTS

ILLUSTRATIONS

TABLES

CHAPTER 1

INTRODUCTION

As an attempt to reduce nickel battery weight, the nickel composite electrode (Ni. C. E.), has been under development in our laboratory since 1978.[1,2] Results of charge-discharge cycling tests on these electrodes showed that the Ni. C. E. can last as long as any other powder sintered nickel plate and has energy densities (Ah/Kg) over 50 percent higher (175 Ah/Kg) than the commercial powder sintered nickel plate. Despite the successes, the composite electrode suffered one major drawback, i.e., an incomplete or very slow rise in utilization of the $Ni(OH)_2$ active material with cycling. Typically, it took 25 - 60 cycles to utilize 90 percent of the active material containing $Co(OH)_2$ as an additive when the composite plaque was loaded electrochemically under the conditions optimized for the powder sinter.

This investigation was originally aimed at finding the electrochemical impregnating conditions that lead to quick utilization of the active material in composite plaques. In the beginning of the investigation, it was surmised that the poor utilization of the active material in the composite plaques could be due to the employment of the electrochemical impregnating conditions which were optimized for powder sintered plaques. Thus, a major effort in the earlier investigation was directed to modify the electrochemical impregnating conditions and to test different impregnating methods to achieve quick, complete loading of the active material in the composite electrode. Naturally, the scope of the investigation was expanded to encompass the efficiency of various loading methods, with emphasis on the electrochemical method.

The interrelationship between loading and utilization of the active material in the composite plaques is a very complicated subject. The complexity of the problem can be appreciated by observing the factors summarized in Figure 1. The upper block of Figure 1 represents the factors affecting electrochemical impregnation. These are separated into two classes: the first class is plaque related and the second represents the controllable impregnation conditions. The factors in the upper block altogether influence the physical and chemical conditions of the active material produced by the impregnation (lower block). The optimization of these factors must fulfill the following goals: rapid, high loading of active material, and quick, efficient charge utilization with a long-cycle life.

In Chapter 2, the general features of electrochemical impregnation and charge-discharge reactions of nickel positive electrodes are examined. A brief description of experiments is presented in Chapter 3. The test results and

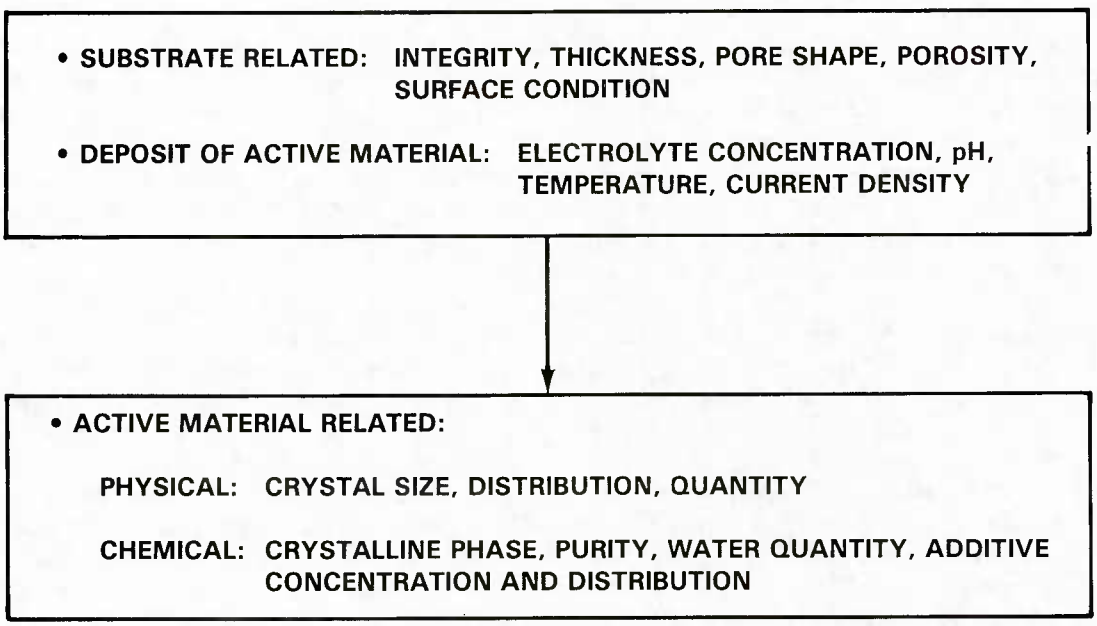

FIGURE 1. FACTORS AFFECTING IMPREGNATION AND UTILIZATION OF ACTIVE MATERIAL. (THE ARROW INDICATES THAT THE UPPER BLOCK INFLUENCES THE LOWER BLOCK)

discussion are divided into two topics: loading efficiency (Chapter 4) and utilization (Chapter 5). The conclusions and recommendations are presented in Chapter 6.

CHAPTER 2

NICKEL POSITIVE ELECTRODE: ELECTROCHEMICAL IMPREGNATION AND BATTERY REACTION

Some basic features of electrochemical impregnation of the nickel positive electrode and its battery reaction in an alkaline cell are examined. The aim of this examination is to provide underlying principles for the discussions in subsequent chapters concerning loading efficiency and utilization rate of nickel composite electrodes. Additional information on this subject matter is reported in detail elsewhere.[3,4]

ELECTROCHEMICAL IMPREGNATION OF NICKEL SUBSTRATE

Electrochemical impregnation is electrochemical precipitation. Unlike chemical impregnation in which hydroxyl ions (OH^-) are provided by an external chemical agent, electrochemical impregnating methods use OH^- ions produced electrochemically at the nickel cathode. When the solubility product, Ksp, of the ions, $[Ni^{2+}] \cdot [OH^-]^2$, exceeds a certain value (8.3×10^{-18}), $Ni(OH)_2$ starts to precipitate. This is shown schematically in Figure 2.

In Figure 2 the abscissa represents the distance from the electrode surface in microscopic scale. The electrode surface can be taken anywhere throughout a porous electrode. The ordinate represents either the concentration of electrolyte ions or their product. The art of good electrochemical impregnation lies in making the region of $Ni(OH)_2$ precipitation as close as possible to the plaque surface and in not allowing this region to spread out from the plaque surface. This is achieved by balancing the rate of production and outward transport of OH^- ions with the rate of inward transport of Ni^{2+} in such a way that the solubility product of the nickel hydroxide exceeds the maximum value only in the region very near the surface during impregnation. This is an extremely difficult task considering the fact that the electrode changes its internal structure as impregnation progresses, affecting the rate of transport of ions. In addition, the diffusion rates of OH^- and Ni^{2+} ions are very much different.

The solubility products, Ksp, of $Ni(OH)_2$ and $Co(OH)_2$ can be calculated based on the following equations:

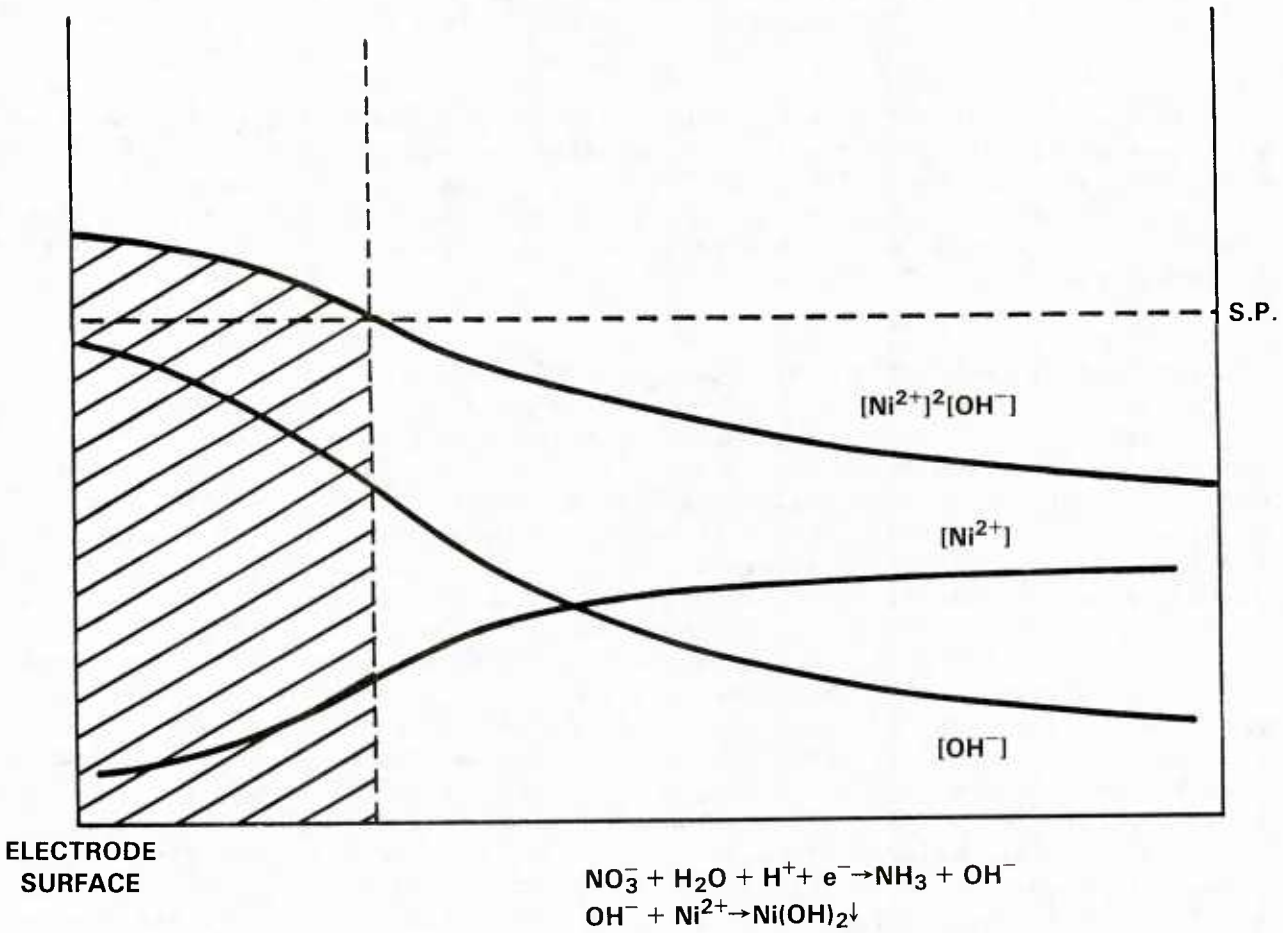

FIGURE 2. ELECTROCHEMICAL IMPREGNATION OF NICKEL HYDROXIDE. (THE CURVES REPRESENT CONCENTRATION OF ELECTROLYTE IONS OR THEIR CONCENTRATION PRODUCT. IN THE REGION WHERE THE CONCENTRATION PRODUCT EXCEEDS THE SOLUBILITY PRODUCT (S.P.) THE IMPREGNATION TAKES PLACE (SHADED AREA))

$$Co(OH)_2 \rightarrow Co^{2+} + 2OH^- \qquad E^o = -1.01\ V$$

$$Ni(OH)_2 \rightarrow Ni^{+} + 2OH^- \qquad E^o = -0.89\ V$$

$$\Delta G^o = - ZFE^o = -RT \ln Ksp\ .$$

The calculated values are as follows:

$$Ksp\ [(Co(OH)_2] = 8.3 \times 10^{-18}\ ,$$

$$Ksp\ [(Ni(OH)_2] = 8.9 \times 10^{-16}\ .$$

BATTERY REACTION AT NICKEL POSITIVE ELECTRODE

The mechanisms of chemical change during charge of the active material or discharge at nickel positive electrode in alkaline cells and charge transport within the active material are not completely understood. Here, we describe only very general features of the battery reaction leaving out microscopic details.

The reactions taking place at the nickel positive electrode are depicted in Figure 3. The electrode is modeled showing three different physical phases: a current collecting (nickel metallic) substrate, a nickel hydroxide active material layer and continguous KOH liquid electrolyte. The conductivity of the active material changes drastically from that of a conductor (NiOOH) in the charged state to an insulator ($Ni(OH)_2$) in the discharge state.

The electrode reactions during charge-discharge can be summarized by the following two reactions, provided the electrode potential does not shift too far to the cathodic region causing hydrogen gas evolution:

$$Ni(OH)_2 + OH^- \underset{\text{discharge}}{\overset{\text{charge}}{\rightleftharpoons}} NiOOH + H_2O + e^- \qquad (1)$$

and [nickel hydroxide] [adsorbed OH^-] $\rightarrow$ [Nickel hydroxide] + $H_2O + O_2 + e^-$ (2)

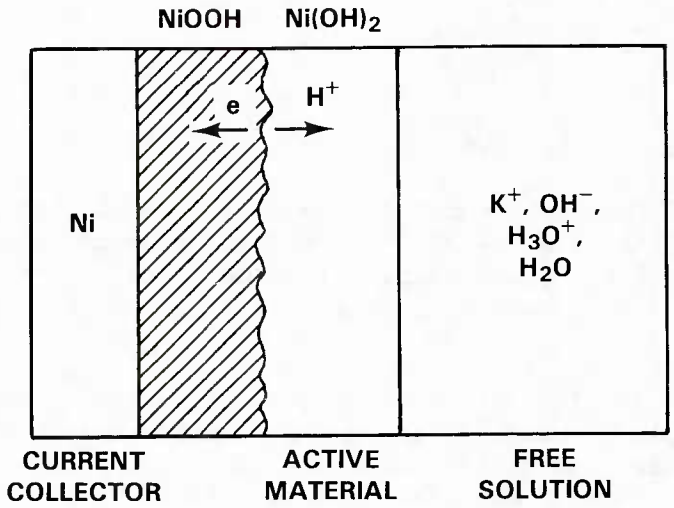

$$[1]\quad Ni(OH)_2 + OH^- \underset{\text{DISCHARGE}}{\overset{\text{CHARGE}}{\rightleftharpoons}} NiOOH + H_2O + e^-$$

$$\left[\begin{array}{l} Ni(OH)_2 \underset{D}{\overset{C}{\rightleftharpoons}} NiOOH + H^+(s) + e^- \\ \\ H^+(s) + OH^-(\ell) \rightarrow H_2O(\ell) \end{array}\right]$$

$$[2]\quad [\text{NICKEL OXIDE}] \cdot 2OH^- \rightarrow [\text{NICKEL OXIDE}] + H_2O + \tfrac{1}{2}O_2\uparrow + 2e^-$$

FIGURE 3. BATTERY REACTIONS AT THE NICKEL POSITIVE ELECTRODE

The reaction (1) is basically a two step process as:

$$Ni(OH)_2 \underset{\text{discharge}}{\overset{\text{charge}}{\rightleftharpoons}} NiOOH + H^+ \text{ (solid)} + e^- \quad (3)$$

$$H^+ \text{ (solid)} + OH^- \text{ (liquid)} \rightarrow H_2O \quad (4)$$

The change of electrode reactions with applied potential is shown in the polarization curves (Figure 4). Unless the potential (with respect to Hg/H_gO reference electrode) falls below 0.0V to generate, hydrogen gas, there are basically two types of reactions, a charge (anodic oxidation)-discharge (cathodic reduction) reaction and oxygen evolution reaction. The reversible potentials of these reactions are denoted as Er and $Er(O_2)$, respectively. At potentials near 0.36V, the current due to oxygen evolution and the discharging current (cathodic reduction) has the same magnitude (i_d), analogous to the mixed potential in corrosion (Em). The reversible potential for charging (anodic oxidation) and discharging current (Er) is approximately 0.38V. It is easily seen in Figure 4 that the charging current exceeds the current due to oxygen evolution (its reversible potential is denoted as $Er(O_2)$) only when the electrode potential lies in the far anodic region near 0.45V.

The efficiency of active material utilization depends partly on how to reduce the waste of electrical work done in oxygen evolution. As noted in Figure 4, unless the electrode potential during the charging reaction is near 0.45V, oxygen evolution is the dominent process. Thus, it is necessary to raise the current density to ensure completion of the charging process. One of the major roles of additives such as cobalt hydroxide in the active material is to raise the oxygen overpotential, so that the waste of electrical work due to oxygen evolution is greatly reduced. Additives are also believed to influence the rate of the charge-discharge reaction. As noted above, the charge and discharge reactions are multi-step processes. It is not clearly understood at what stage of the process the additives become directly involved. However, there are indications that the additive effect is a surface phenomena[5] rather than a bulk effect. Another important function of the additives is to prevent the coagulation of nickel hydroxide particles, so that their surface area is not reduced.[6]

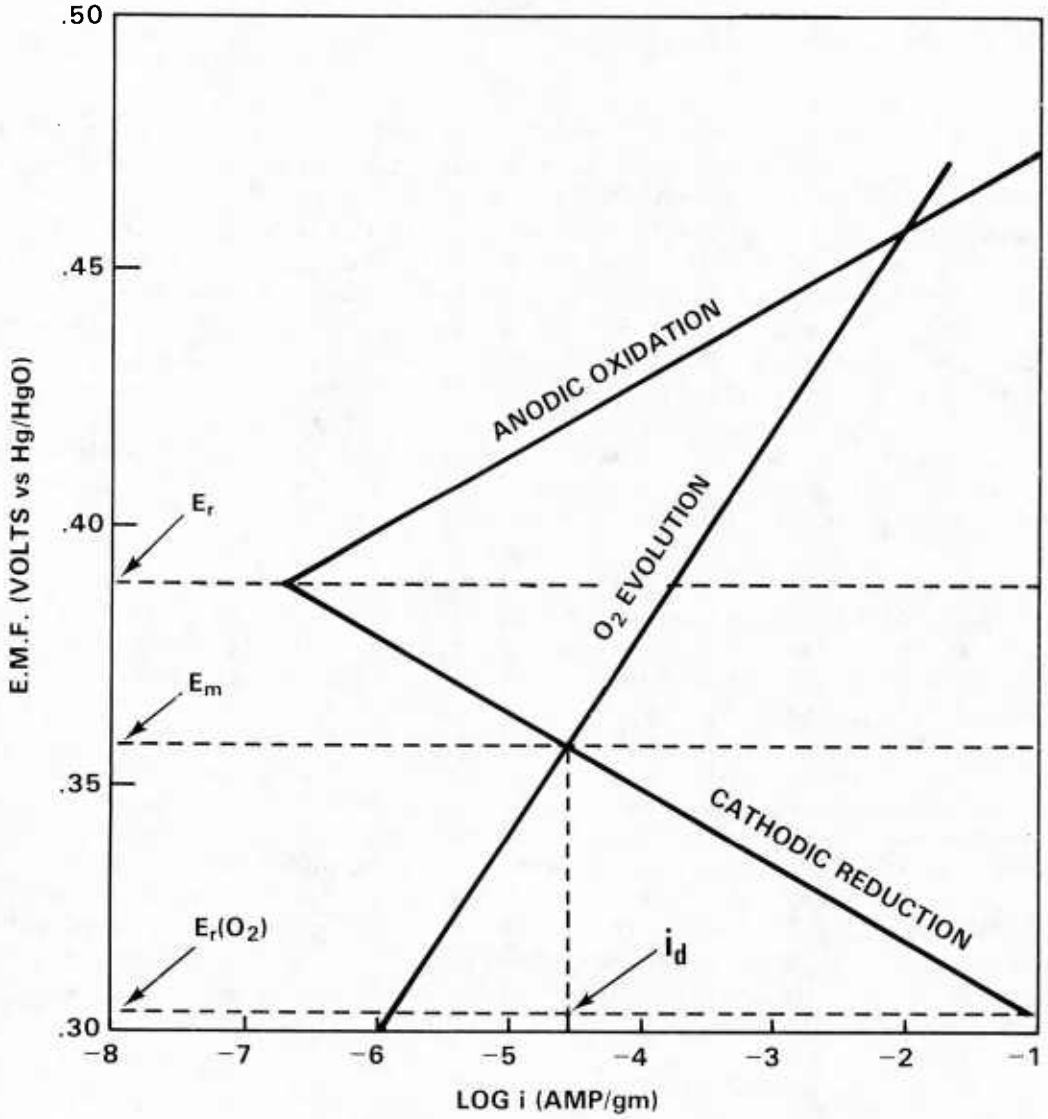

FIGURE 4. POLARIZATION CURVES FOR CHARGE-DISCHARGE AND OXYGEN EVOLUTION REACTIONS AT NICKEL POSITIVE ELECTRODE

CHAPTER 3

EXPERIMENTAL

Experimental details of the nickel composite plaque fabrication, electrochemical impregnation and cycling test have been given in the first technical report[7] of this series. Only additional features are described here.

PHYSICAL DESCRIPTION OF THE ELECTRODE

Composite plaques in four different thicknesses, 30 mils (0.75 mm), 40 mils (1.02 mm), 60 mils (1.52 mm), 100 mils (2.54 mm), were cut into smaller pieces with dimensions of 2.3 x 4.5 cm or 4.5 x 7.0 cm for impregnation and cycling tests. Porosity of the composite plaques ranged between 80 - 85 percent.

IMPREGNATION OF NICKEL HYDROXIDE ACTIVE MATERIAL

Electrochemical Impregnation

The electrochemical method applied was basically that of Pickett.[8] His adaptation uses a 1:1 mixture of water and ethanol as the solvent. During impregnation, either constant potential or constant current control was used to regulate the cathode reaction. A constant potential was applied between the cathode (the composite plaque under impregnation) and the anode (nickel sheet electrode) by using the remote sensing feature of a DC power supply. This circuitry eliminates IR drop in the leads for high current application.

Concentrations of Ni^{2+} and Co^{2+} (7 wt percent of the Ni^{2+} concentration) ions in the impregnating bath were monitored by using a CARY 16 Spectrometer.

pH Control

The experimental setup for controlling the pH is illustrated in Figure 5. The pH of the impregnating bath was regulated by adding dilute HNO_3 when the pH of the bath reached a preselected upper pH limit. This was accomplished by connecting a pH electrode (Ingold combined with temperature range between 0 to 100°C) in the bath to a pH controller (Horizon Ecology Model 5997-20) which sends an activation signal to a dispenser when the bath pH reaches the

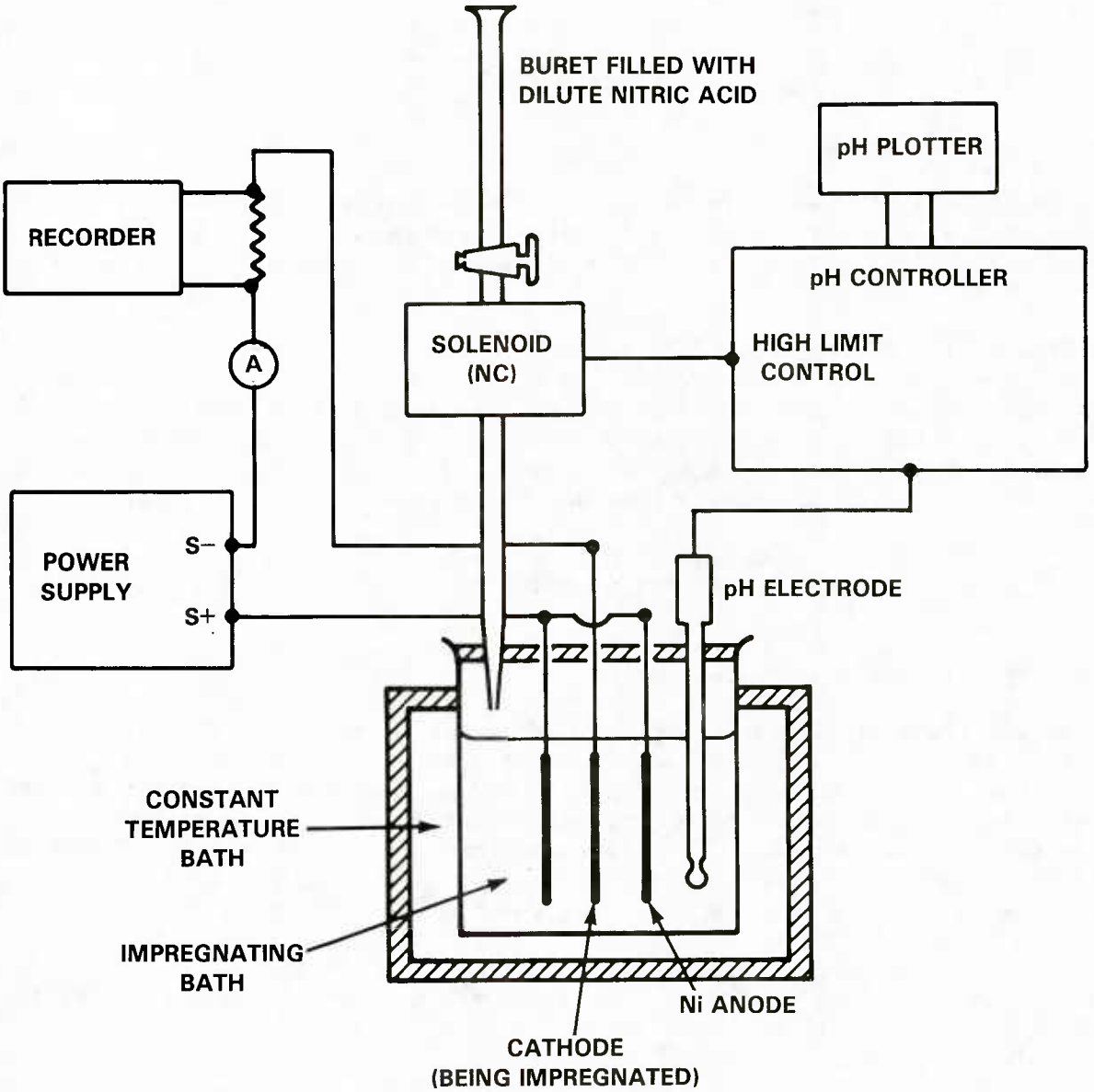

FIGURE 5. pH CONTROL IN ELECTROCHEMICAL IMPREGNATION

preselected upper limit. The dispenser delivers the dilute HNO_3 directly into the bath on demand when the solenoid valve attached to the tip of a buret containing the acid is activated. The bath pH was controlled to within 0.5 pH units.

Chemical Impregnation

Chemical impregnation of the composite plaque was carried out following the polarization method.[9] The impregnating solution was prepared by dissolving about 400 grams of nickel nitrate ($Ni(NO_3)_2 \cdot 6H_2O$) and 28 gm of cobalt nitrate ($Co(NO_3)_2 \cdot 6H_2O$) in 250 ml of distilled water. A composite plaque was placed in a vacuum dessicator which was evacuated using a rotary pump (< 40 mm Hg) for about 20 minutes. The impregnating bath then was introduced through a funnel to the dessicator. Immediately after soaking, the plaque was transferred to a hot 20 percent KOH solution (80 to 100°C). The composite plaque was placed between two nickel sheet counter electrodes. About 8 A/dm^2 cathodic current was applied to the composite plaque cathode for 20 minutes. The anode-cathode distance was one-half inch. These procedures were repeated several times until there was no further weight gain.

Direct Loading (Suspension Method)

The active material used for suspension impregnation[10] was prepared by mixing commercial battery grade $Ni(OH)_2$ (which already contains 2 wt. percent of cobalt metal powder) uniformly with 5 wt. percent of reagent grade $Co(OH)_2$. This mixed material was suspended in ethylene glycol and the resulting fluid was forced into the open structure of the composite plaque. Light pressing of the fluid into the plaque and removal of the ethylene glycol were repeated several times until the desired weight gain (loading) was achieved.

Post-Impregnation Additive Addition (Surface Treatment)

Post-impregnation additive addition was made by cathodically depositing a thin layer of $Co(OH)_2$ on the surface of the active material in the composite body (either pure cobalt or pure nickel electrode was used as the anode). Either 1.8M $Co(NO_3)_2$ or 0.5M cobalt acetate solution in a 1:1 mixture of water and ethanol was used as the impregnating bath with the temperature maintained at 50°C during impregnation. Depending upon the desired thickness of of the $Co(OH)_2$ film, the impregnation time was adjusted from 10 seconds to 2 minutes and the current density was 50 mA/cm^2.

The $Co(OH)_2$ film can also be formed chemically by soaking the impregnated electrode in the cobalt compound solution followed by alkaline agent treatment after the solution is drained off.

CHARGE-DISCHARGE CYCLING

Details of the cycling arrangement were given in the previous report.[7] Test cells were fabricated using a single nickel composite electrode sandwiched

between two commercial cadmium electrodes to produce a positive limiting condition. No additive was added to the 31 percent KOH electrolyte. One complete cycle in the continuous cycling tests included charging at the C rate for 80 minutes, 10 minutes rest, followed by discharge at C/2 rate to 1.0V cutoff. Theoretical total charge capacity of the nickel electrode was determined by the weight gain after impregnation.

CHAPTER 4

LOADING EFFICIENCY OF ACTIVE MATERIAL

ELECTROCHEMICAL IMPREGNATION

As previously mentioned, the efficiency of electrochemical impregnation depends upon the concentration profiles of Ni^{2+} and OH^- ions near the nickel plaque surface. Factors determining the production and transport of these ions include: pH, temperature and Ni^{2+} ion concentration of impregnating bath, current density, and mechanical agitation of the bath. The effects of these factors on loading yield and efficiency are discussed in this section. Unless stated otherwise, the normal physical plaque parameters were: thickness - 30 mils (0.762 mm), porosity - 85 percent.

Mechanical Stirring

When the impregnating bath was agitated with a magnetic stirrer, the loading of active material was very much reduced regardless of pH, current density or the duration of impregnation (Table 1). It is seen in Table 1 that plaques (No. 1 to No. 4) impregnated in the agitated bath have a low loading level of the active material regardless of the bath pH. Plaque No. 5 impregnated without agitation has a loading level more than three times higher than that of plaque No. 3 and more than *ca.* fourteen times higher than that of plaque No. 2. This result clearly indicates the adverse effect of stirring on loading efficiency. The rapid movement of the bulk solution, as the magnetic bar rotates, washes away OH^- ions accumulated in the close vicinity of the inner surface of the composite plaques and thus hinders the ready precipitation of $Ni(OH)_2$. The powdersinter (No. 6) is not affected by stirring because of its much smaller pore size. As the result of this experiment, all further impregnations of the composite plaques did not use mechanical stirring.

pH of Impregnating Bath

Although the loading level is low, the effect of pH on loading efficiency can be observed from Table 1. After a sudden rise around pH 3, the loading level becomes constant with increasing pH. For composite plaques impregnated in a 1.8M and 3.5M Ni^{2+} solution, the optimum pH was 4 and 3, respectively.

Current Density and Nickel Concentration

The effect of cathodic current density (mA/cm^2) and nickel concentration of the bath on loading level (gm/cm^3) is presented in Figure 6. The loading

TABLE 1. EFFECT OF THE MECHANICAL STIRRING ON THE LOADING OF THE ACTIVE MATERIAL

Plaque No.	Stirring (Yes or No)	Initial Weight (gm)	Impregnation Conditions pH	Weight Gain (gm)
1	Y	1.052	2.0-3.0	0.020
2	Y	1.026	2.5-3.0	0.033
3	Y	1.032	3.0-3.5	0.143
4	Y	1.025	3.5-4.0	0.166
5	N	1.025	2.8-3.2	0.474
6*	Y	1.853	2.8-3.2	0.509

*Commercial powder sintered plaque.
Total duration of impregnation is 1 hour.
Current density: 55 mA/cm^2

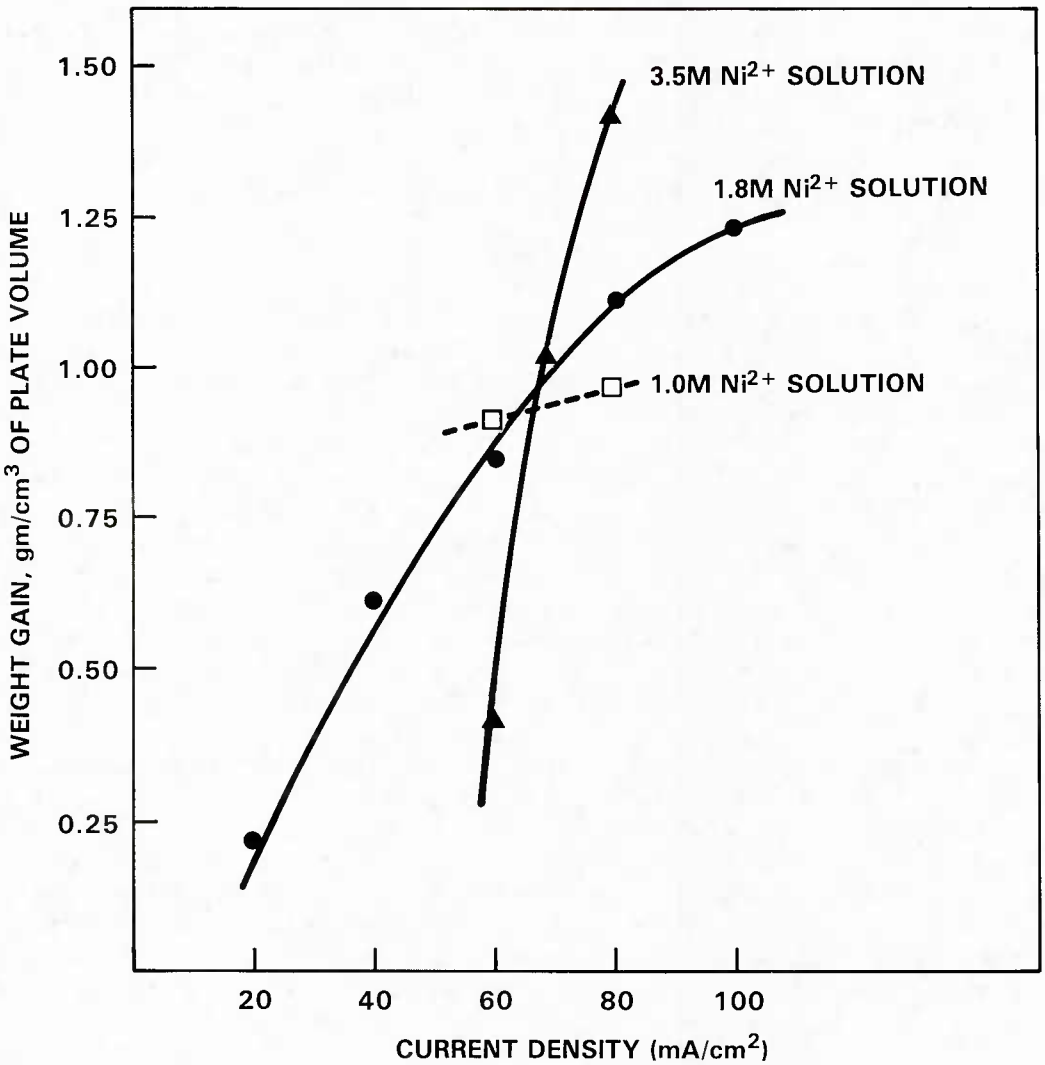

FIGURE 6. EFFECT OF CURRENT DENSITY AND NICKEL CONCENTRATION ON LOADING EFFICIENCY

level is expressed in terms of weight gain of composite plaques after 1 hour of constant current impregnation. Figure 6 shows that the weight gain curve is much more sensitive to the cathodic current density as the Ni^{2+} concentration increases. For a 1.0M Ni^{2+} solution the effect of current density is not profound, whereas for a 3.5M Ni^{2+} solution the weight gain curve is almost linear in the region between 60 and 80 mA/cm^2. For a 1.8M Ni^{2+} solution the weight gain curve levels off as the current density exceeds 100 mA/cm^2.

The loading of active material into the composite plaques of 82 percent porosity from an impregnating bath containing 1.8M Ni^{2+} and 3.5M Ni^{2+} solutions was complete with a weight gain of about 1.6 gm/cm^3 of plate volume. To achieve this loading level it takes about 1 hour for the plaques impregnated in 3.5M Ni^{2+} solution and about 2 hours for the plaques impregnated in 1.8M Ni^{2+} solution with 80 mA/cm^2 current density for both cases.

The reason why the effect of current density is not profound in a 1M Ni^{2+} solution bath is possibly because the limiting factor is the nickel concentration. The sharp weight gain curve with the increase of current density for impregnations in a 3.5M Ni^{2+} is attributed to an increase in the production rate of OH^- ions and to an increase in the conductivity of the solution. The specific conductivity of 1M, 1.8M, and 3.5M solutions are 0.033, 0.049, and 0.033 $ohm^{-1}\ CM^{-1}$, respectively (Table 2). Addition of 7 percent Co^{2+} to the solution does not affect the values significantly. The increase in the rate of OH^- generation as the current density increases compensates for the lower pH of 3.5M Ni^{2+} solution. For the 3.5M Ni^{2+} solution, the increase of current density from 60 to 80 mA (per cm^2 of projected electrode area) increases the loading level by more than a factor of three. At current densities above 60 mA cm^{-2}, the loading level of a 3.5M Ni^{2+} solution is higher than the loading level of a 1.8M Ni^{2+} solution.

The optimized current density (in terms of loading level) for the composite electrode in a 1.8M Ni^{2+} solution is around 80 mA cm^{-2} which is higher than the value for powder sinter ($\sim$ 50 mA cm^{-2}).[11] This difference is greater if the current density is normalized by the real surface area for both plaques (the composite plaque has only 30 percent the surface area of the powder sinter for the same plaque volume). The higher current density required for impregnating the composite plaque is due to its higher electrical resistivity ($\sim$ 800 $\mu\Omega \cdot$ cm) which is greater that that of the powder sinter (200 $\mu\Omega \cdot$ cm).

It has been shown that the impregnation in a 3.5M Ni^{2+} solution achieves a faster (time) loading of the active material than in a 1.8M Ni^{2+} solution, but has associated with it a higher risk of active material deposition on the plaque surface. Therefore, the optimization process in the subsequent experiments was focused to find the impregnation conditions that minimize such deposition while the conditions such as the Ni^{2+} concentration (3.5M), pH (3) and the bath temperature (85°C) were held constant.

Constant Potential Impregnation (3.5M Ni^{2+} Solution)

Accumulation of surface deposit is detected by monitoring the potential (vs. anode) of the composite plaque during constant current impregnation

TABLE 2. CONDUCTIVITY OF IMPREGNATING SOLUTIONS AT T = 22.3°C MEASURED BY IMPEDANCE BRIDGE METHOD

Type of Bath*	Resistivity ρ ($\mu\Omega \cdot cm$)	Conductivity k (Ω^{-1} cm^{-1})
1.0M $Ni(NO_3)_2$ with 7% $Co(NO_3)_2$	30.3	0.033
1.8M $Ni(NO_3)_2$ with 7% $Co(NO_3)_2$	20.6	0.049
1.8M $Ni(NO_3)_2$ with no $Co(NO_3)_2$	18.7	0.053
3.5M $Ni(NO_3)_2$ with 7% $Co(NO_3)_2$	30.4	0.033

*Solvent is a 1:1 mixture of water and ethanol.

(Figure 7). A sudden increase in potential is indicative of heavy surface deposit. As a way to minimize this type of deposition, a constant potential control was used instead of constant current. The advantage of the constant potential control is that the precipitation front, as it moves toward the plaque surface, slows down as the current density increases. In a strict sense, the control of potential should be with respect to a reference electrode rather than the anode whose condition changes during the course of impregnation.

The results of constant potential impregnation in a 3.5M N_i^{2+} solution are presented in Table 3. Table 3 shows that increased initial current density substantially reduces the impregnation time required to achieve a given loading level of the active material. For example, when the potential was increased from -2 to -3V (approximately), the impregnation time was reduced from 80 to 16 minutes. However, there is an increased danger that the active material will be deposited on the outer surface of plaques before filling the inside as the potential is increased. The measurements of electrode thickness after impregnation indeed showed that surface deposition took place with the higher potential impregnation even though the impregnation time was reduced.

The onset of heavy surface deposits can be detected by monitoring the current profiles during impregnation as shown in Figure 8. The figure shows how current density changes as impregnation procedes. As the potential is set higher, the current density has a higher initial value but declines faster. Each curve has an inflection point associated with it. It was found by examination that deposition of the active material takes place on the surface of the composite plaque in the time after the inflection.

No attempts were made to shorten the impregnation time in a 1.8M Ni^{2+} solution. Constant potential impregnation in this solution (with 80 mA $\cdot$ cm^{-2} initial current density) showed a loading level close to that achieved by constant current impregnation. It is notable that during the impregnation, a current oscillation was observed as shown in Figure 9. The oscillation may indicate a periodic precipitation of $Ni(OH)_2$ active material. However, its exact cause has not yet been determined. Such behavior was not observed in the impregnations carried out in a 3.5M Ni^{2+} solution.

Intermittent Current and Temperature Effects

In order to prevent a fast movement of the precipitation front during impregnation in a 3.5M Ni^{2+} solution, two experimental modifications were made to the continuity of current flow and the bath temperature while employing the constant potential impregnation. First, the power supply for impregnation was switched off peridically. During the power-on period the potential is constant, while the current decreases as impregnation takes place. During the power-off period the current is zero. This periodic switching-off of the power supply established intermittent current flow. Second, the bath temperature was lowered. These modifications were directed toward suppressing the production rate of OH^- ions and impeding the transport of Ni^{2+} and OH^- ions.

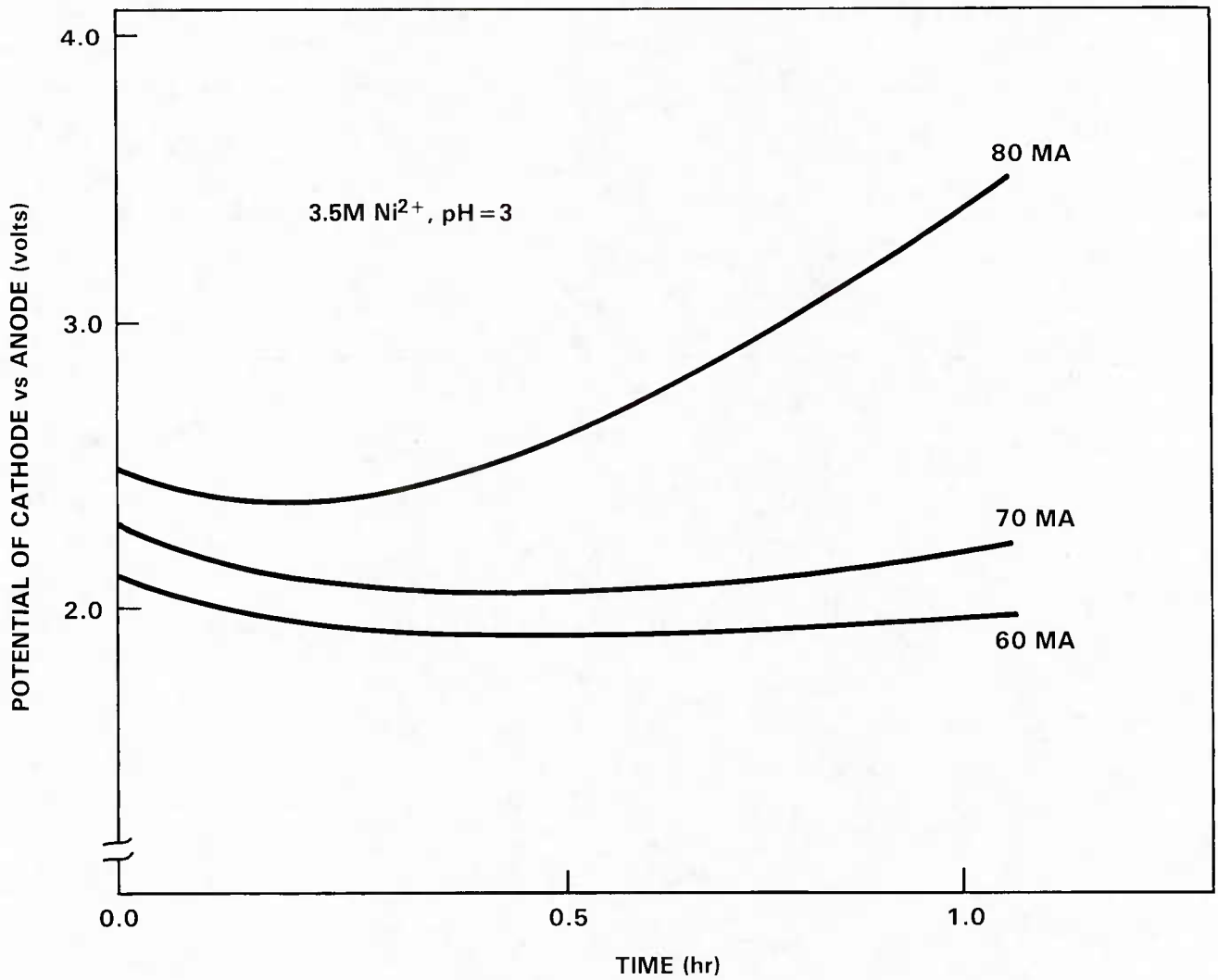

FIGURE 7. ELECTRODE POTENTIAL (CATHODE VERSUS ANODE PROFILE DURING CONSTANT CURRENT IMPREGNATION

TABLE 3. LOADING EFFICIENCY OF CONSTANT POTENTIAL IMPREGNATION (3.5M Ni^{2+} SOLUTION)

Electrode No.	Applied Potential (V)	Initial Current Density (mA/cm^2)	Impregnation Time (Minutes)	Weight Gain (gm/cm^3 of plate volume)
36	-2.05	100	80	1.37
35	-2.26	150	44	1.47
42	-2.58	200	30	1.39
45	-3.27	300	16	1.34

*pH of the bath: 2.5 - 3.0.

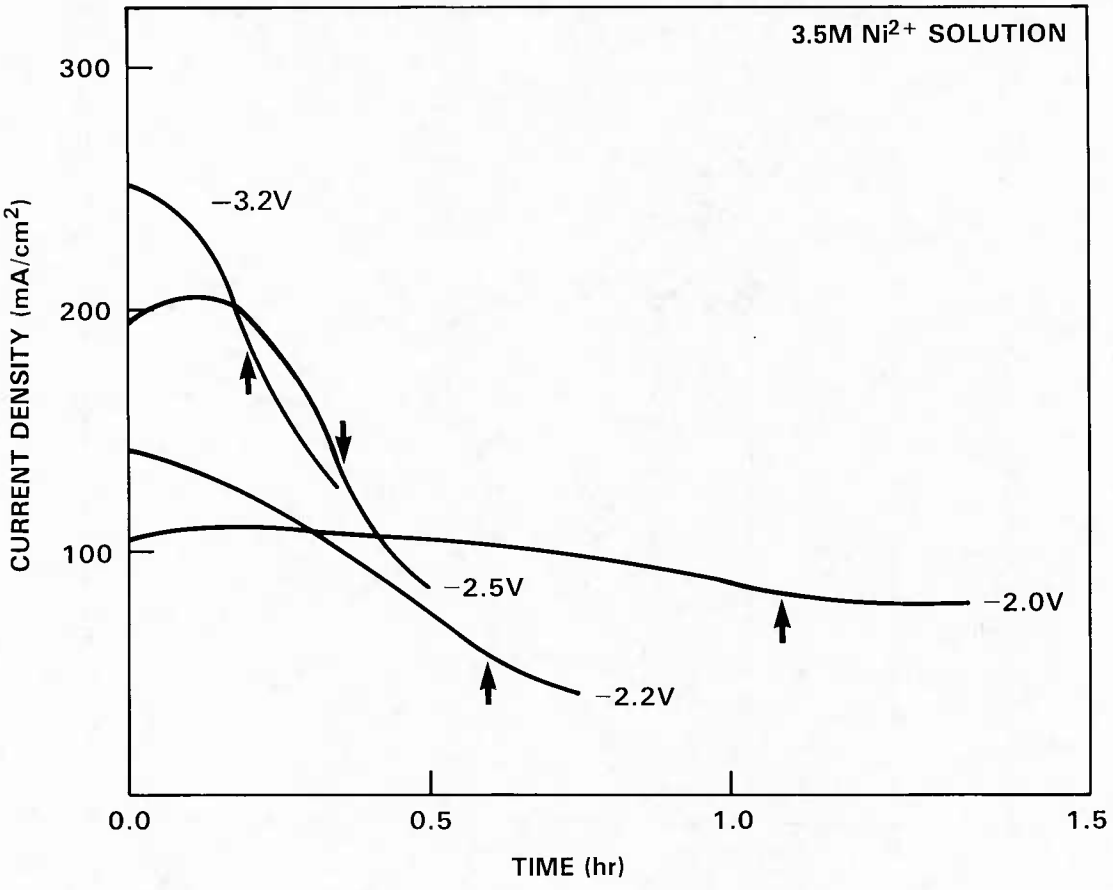

FIGURE 8. CURRENT DENSITY PROFILE OF IMPREGNATING CELL (3.5M Ni^{2+} SOLUTION) DURING CONSTANT POTENTIAL IMPREGNATION. (THE POTENTIAL ON EACH CURVE DENOTES THE POTENTIAL OF CATHODE VERSUS ANODE. THE ARROWS INDICATED INFLECTION POINT OF EACH CURVE)

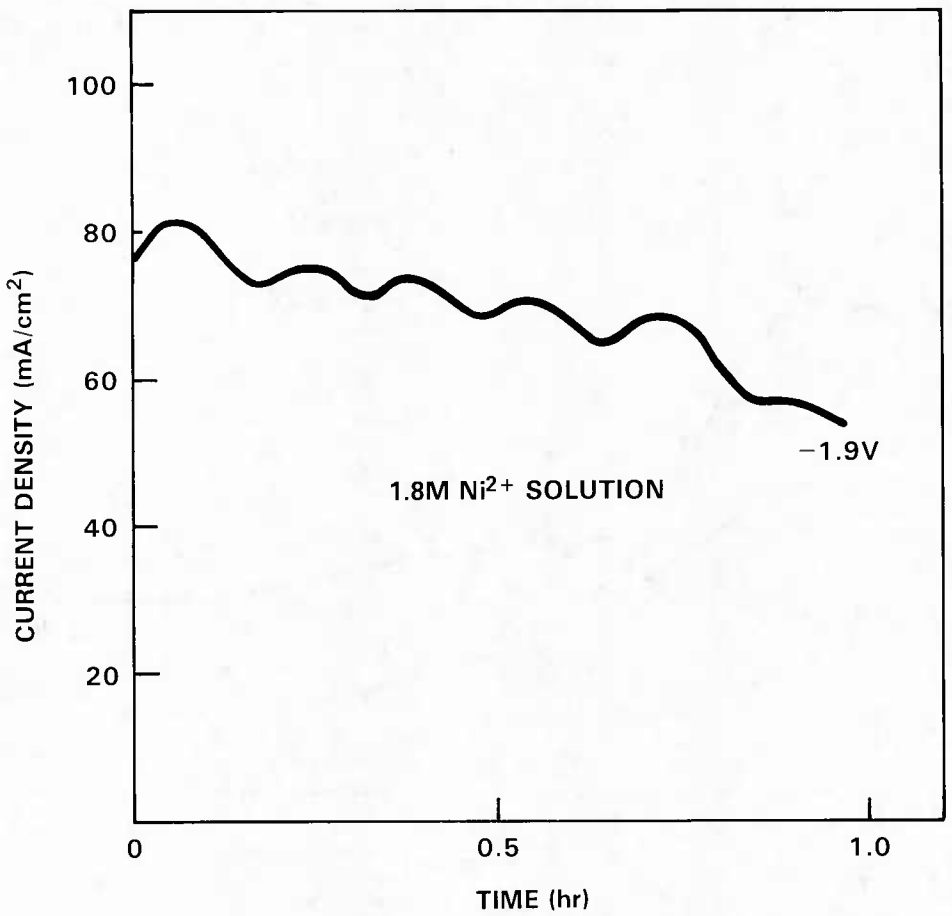

FIGURE 9. CURRENT DENSITY OSCILLATION OF IMPREGNATING CELL (1.8M Ni^{2+} SOLUTION) DURING CONSTANT POTENTIAL IMPREGNATION. (THE CATHODE POTENTIAL = −1.9V)

The current interruptions during constant potential impregnation were made in three different modes:

Mode 1. - A period of 1 minute power-on followed by 1 minute power-off repeating for 60 minutes (net 30 minutes power-on).

Mode 2. - A period of 6 minutes power-on followed by 6 minutes power-off repeating for 60 minutes (net 30 minutes power-on).

Mode 3. - A continuous power-on for 30 minutes without interruption.

The total impregnation time for modes 1 and 2 was 60 minutes (net 30 minutes power-on). The initial current density was set at 80 mA/cm^2. The dependency of loading level on bath temperature and duration of potential applied are shown in Figure 10.

At 25°C, the impregnations with an intermittent current yielded higher loadings than impregnations with the continuous power-on, whereas the trend was reversed at higher temperatures (over 55°C). In mode 3 impregnations (continuous current), the lowest loading occurred at 25°C, while in mode 1 impregnations the lowest loading took place at 85°C. Although the highest loading was achieved at 55°C in mode 3 impregnations, the plaques impregnated at this temperature showed a thick deposit of the active material on the outer surface of the plaques. The plaques impregnated at 25°C did not exhibit any significant deposit on the plaque surface.

How the impregnation with intermittent current at 25°C increases the loading of active material is not clearly understood. A possible explanation is that during the power-off period Ni^{2+} and NO_3^- ions gain time to readjust their concentration profile throughout the porous body so that the rate of OH^- production and the rate of $Ni(OH)_2$ precipitation is increased in the region close to the inner surface of the plaques. A lower rate of production and transport of OH^- ions at 25°C was observed by monitoring the pH of the impregnating bath. The pH even decreased during impregnation at this temperature.

Increasing the bath temperature results in an increase not only in the rate of inward transport of Ni^{2+} ions from the bulk solution (bath) to the plaque pores, but also, even to a greater degree, in the rate of outward transport of OH^- ions because of their larger diffusion constant. Therefore during the power-off period, OH^- ions produced during the power-on period diffuse out rapidly. The concentration of the ions required for $Ni(OH)_2$ precipitation does not exceed the K_{sp} of $Ni(OH)_2$. Hence, mode 1 impregnations with the shortest period of power-on and -off resulted in the lowest loading at 85°C.

Plaque Thickness

The dependency of loading level of the active material into the composite plaque on the plaque thickness is presented in Table 4. The impregnation was made in a 1.8M Ni^{2+} solution. It is seen that the loading level per unit volume of the composite plate does not decrease with increase of plaque thickness. The average weight gain is about 1.45 gm/cm^3 of plate volume. It takes about 50 percent more time to impregnate thick plaques (over 1.5mm) than thin plaques to achieve similar loading levels.

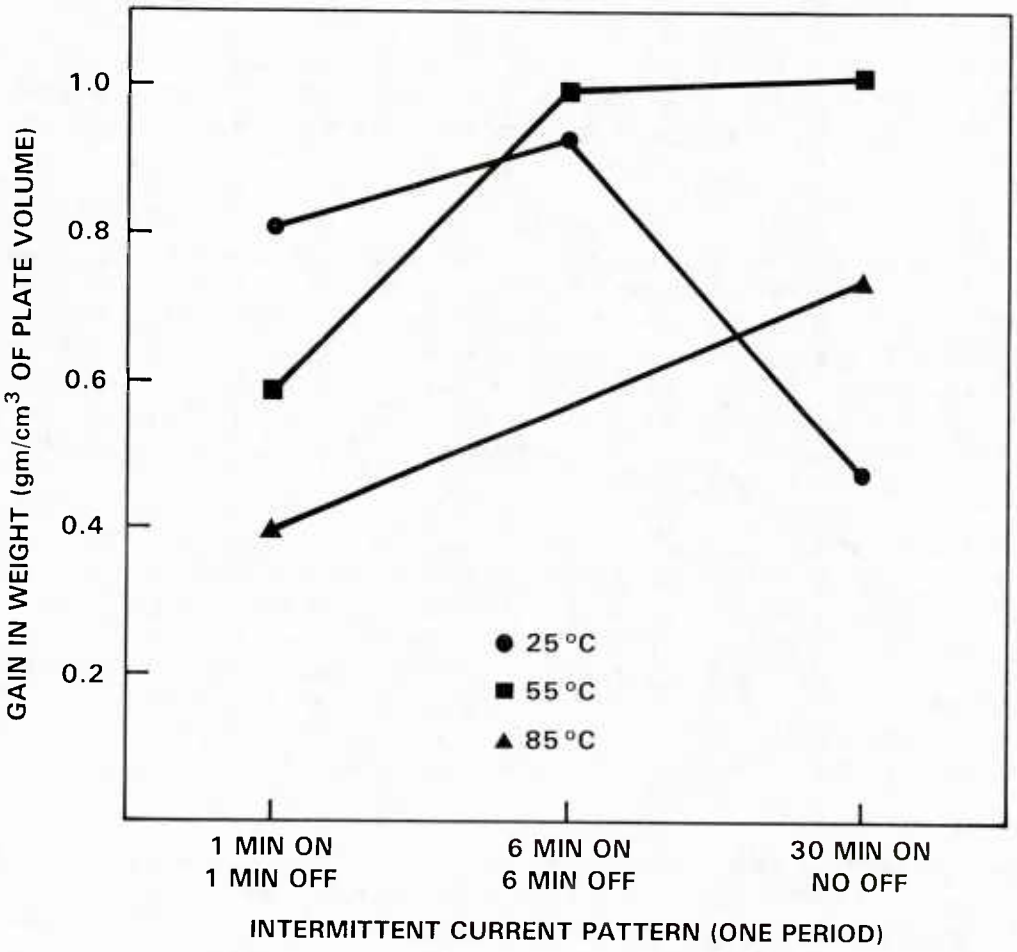

FIGURE 10. EFFECT OF INTERMITTENT CURRENT APPLICATION AND BATH TEMPERATURE OF IMPREGNATING BATH ON LOADING EFFICIENCY (3.5M Ni^{2+} SOLUTION). (THE NET IMPREGNATING TIME IS 30 MINUTES)

TABLE 4. DEPENDENCE OF LOADING LEVEL ON THE COMPOSITE PLAQUE THICKNESS

Plaque No.	Thickness (mm)	Duration of Impregnation (Minutes)	Loading Level (gm/cm^3 of plate volume)
23	0.75	90	1.52
26	1.02	90	1.44
75	1.52	120	1.33
27	2.54	120	1.40

Concentration of Impregnation solution = 1.8M Ni^{2+} (7% Co^{2+})

pH = 4.0

Current density = 80 mA/cm^2

CHEMICAL IMPREGNATION (POLARIZATION METHOD)

The loading yield in the nickel composite plaque by the polarization method is presented in Table 5. The yield of the composite plaque is very close to the reported values for powder sinter.[9] For the optimization of loading efficiency, it is not advantageous to use the chemical impregnation method because of its cumbersome preparation processes.

SUSPENSION METHOD

Probably one of the greatest advantages of the composite substrate lies in the possiblity of loading the externally prepared active material. The advantage of this method is mainly three fold: no involvement of nitrate (NO_3^-) ion, homogeneous mixing of active material [$Ni(OH)_2$] and additive [$Co(OH)_2$], and the possible reduction of cost and time. The loading yield with this method is presented in Table 6 and is very comparable to both chemical and electrochemical methods.

TABLE 5. LOADING OF COMPOSITE PLAQUE BY CHEMICAL IMPREGNATION

(a) Initial Plaque Weight: 2.44 gm (0.75 mm thickness)

Impregnation Cycle No.	Gain in Weight (gm)	Cumulative Gain in Weight (gm)	Gain in Weight, gm/cm^3 of Plate Volume
1	0.84	0.84	0.288
2	0.69	1.53	0.524
3	0.50	2.03	0.695
4	0.58	2.61	0.894
5	0.53	3.14	1.075

(b) Initial Plaque Weight: 3.28 gm (0.75 mm thickness)

Impregnation Cycle No.	Gain in Weight (gm)	Cumulative Gain in Weight (gm)	Gain in Weight, gm/cm^3 of Plate Volume
1	0.91	0.91	0.278
2	0.73	1.64	0.502
3	0.68	2.32	0.709
4	0.58	2.90	0.887
5	0.55	3.45	1.055
6	0.63	4.08	1.248

TABLE 6. LOADING OF COMPOSITE PLAQUE BY SUSPENSION METHOD

(a) Initial Plaque Weight: 0.74 gm (1.0 mm thickness)

Impregnation Cycle No.	Gain in Weight (gm)	Cumulative Gain in Weight (gm)	Gain in Weight, gm/cm^3 of Plate Volume
1	0.92	0.92	0.833
2	0.35	1.27	1.150
3	0.01	1.28	1.159

(b) Initial Plaque Weight: 1.16 gm (2.5 mm thickness)

Impregnation Cycle No.	Gain in Weight (gm)	Cumulative Gain in Weight (gm)	Gain in Weight, gm/cm^3 of Plate Volume
1	1.11	1.11	0.404
2	0.97	2.08	0.756
3	0.74	2.82	1.025
4	0.16	2.98	1.084

CHAPTER 5

UTILIZATION OF ACTIVE MATERIAL

As stated in Chapter 1, the composite electrode exhibited an incomplete or slow rise in utilization of the $Ni(OH)_2$ active material with cycling. One of the main objectives of this investigation was to shorten the number of cycles required to achieve full utilization.

The lower utilization rate of the composite electrode can be partly explained by the potential drop across the active material in the large pores (peak value of pore diameter, 55 μm, about five times larger than that of powder sinter)[2] of the composite electrode. However, this utilization loss, which was found to be approximately 10 percent of the maximum utilizable charge, is an inherent characteristic of the composite electrode. It is not the main issue addressed in this report. The main cause of the sluggish utilization rate is attributed to inefficient use of the additive, because a homogeneous distribution of additive throughout the active material is difficult to achieve with the increased pore size. The adverse effect of maldistributed additive (such as in the form of isolated patches) on the utilization of the active material becomes more severe with the increase of the pore size. Our efforts to unravel the relationship between the activity of the additive and its distribution in the sintered composite electrode are described in this chapter.

CLASSIFICATION OF UTILIZATION RISE CURVES OF COMPOSITE ELECTRODES

Definition of Percent Utilization

The percent utilization of the charged active material during a discharge cycle is defined as the ratio of the utilizable charge at that cycle to the total charge. Since the valence change of nickel ions during charge-discharge cycles can be greater than one, the possible maximum utilization can exceed 100 percent. The maximum utilization (or full utilization) of composite electrodes was found to be slightly above 100 percent.

Classification

The first series of the nickel composite electrodes in this study were impregnated by the electrochemical method. $Co(OH)_2$ additive was incorporated into $Ni(OH)_2$ active material by coprecipitation. Test cells using these

nickel electrodes showed a wide variation in utilization during the first 50 cycles. Since the total charge of Cd electrodes far exceeds that of the nickel electrode, the utilization during the initial cycles reflects the characteristics of the nickel electrode. According to the shape of the utilization-rise curve, which shows the relationship between utilization percentage and charge-discharge cycles, the electrodes can be classified into three different groups as shown in Figure 11. Type 1 electrodes exhibit an ideal behavior - quick rise to full utilization and no decrease in utilization with additional cycles. Type 2 electrodes show low utilization and never achieve full utilization even after more than 100 cycles. Type 3 electrodes show a slow, almost linear, rise to a near full utilization requiring from 50 to 100 cycles. In this scheme, electrodes with a heavy surface deposit of active material are not considered.

CAUSES OF NON-IDEAL BEHAVIOR

Inhomogeneity of Additive Distribution

The variance in utilization of the charged, active material during discharge was attributed to the difficulty in achieving a homogeneous additive distribution throughout the active material during electrochemical impregnation. The pore structure of the composite electrodes is characterized by large pore size, a wide distribution of pore diameters, and an irregular pore shape. These factors make it difficult to achieve a uniform current distribution inside the composite body. In addition to probable non-uniform current distribution, the difference in solubility product between $Ni(OH)_2$ and $Co(OH)_2$ can result in a precipitation of $Co(OH)_2$ in isolated patches in the active material.

It was possible to eliminate the inhomogeneous additive distribution, at least, on macroscopic scale, with the suspension press method. Since the active material and additive are premixed before infiltration into the composite substrate in this method, a uniform distribution of additive is virtually ensured. Although the electrodes prepared by this method still showed type 3 behavior, the consistency of their behavior in the utilization rate seems to indicate that some complexities in the behavior associated with the electrodes impregnated by the electrochemical method (coprecipitation) have been eliminated.

Particle Size

As an attempt to achieve ideal utilization behavior, the active material particle size was reduced to achieve a more microscopic homogeneity in the additive distribution. The reduction of the particle size was originally done for a more complete, and even pore filling down to small pores. The particle size of cobalt hydroxide is usually much smaller than nickel hydroxide, producing an inherent small scale inhomogeneity of the additive in the mixture. The effect of particle size on utilization is shown in Figure 12. The $Ni(OH)_2$ particles were ground successively into smaller particles and mixed with

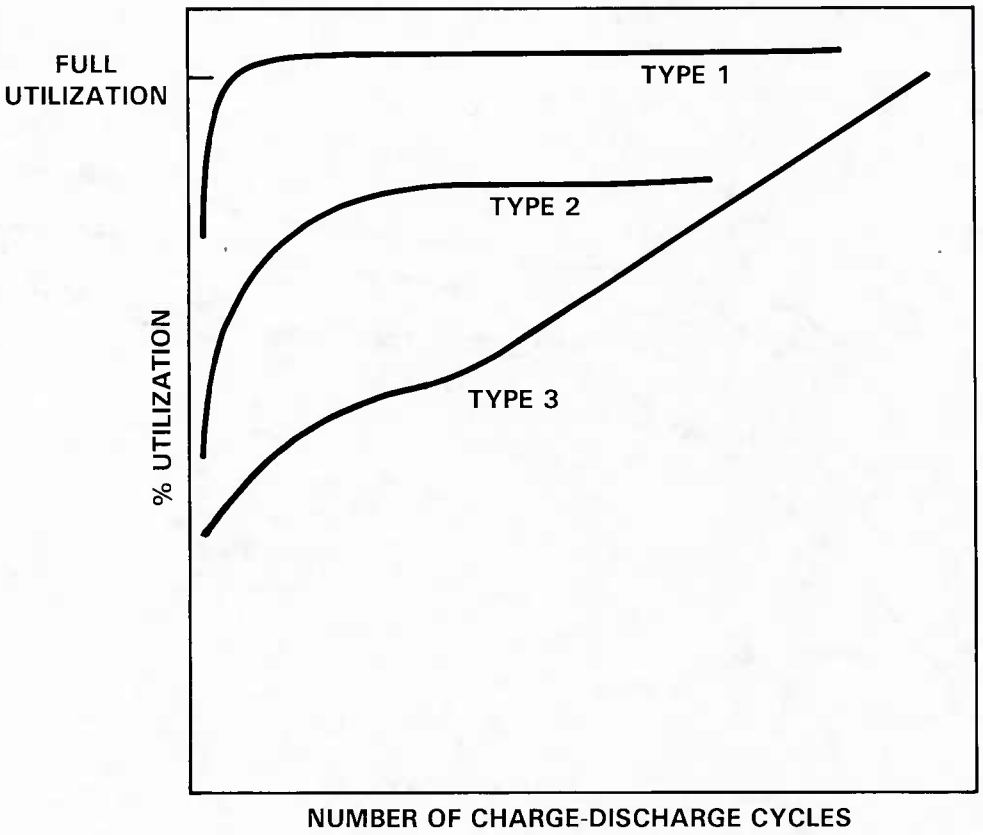

FIGURE 11. CLASSIFICATION OF THE PATTERN OF THE UTILIZATION RISE EXHIBITED IN THE NICKEL COMPOSITE ELECTRODES

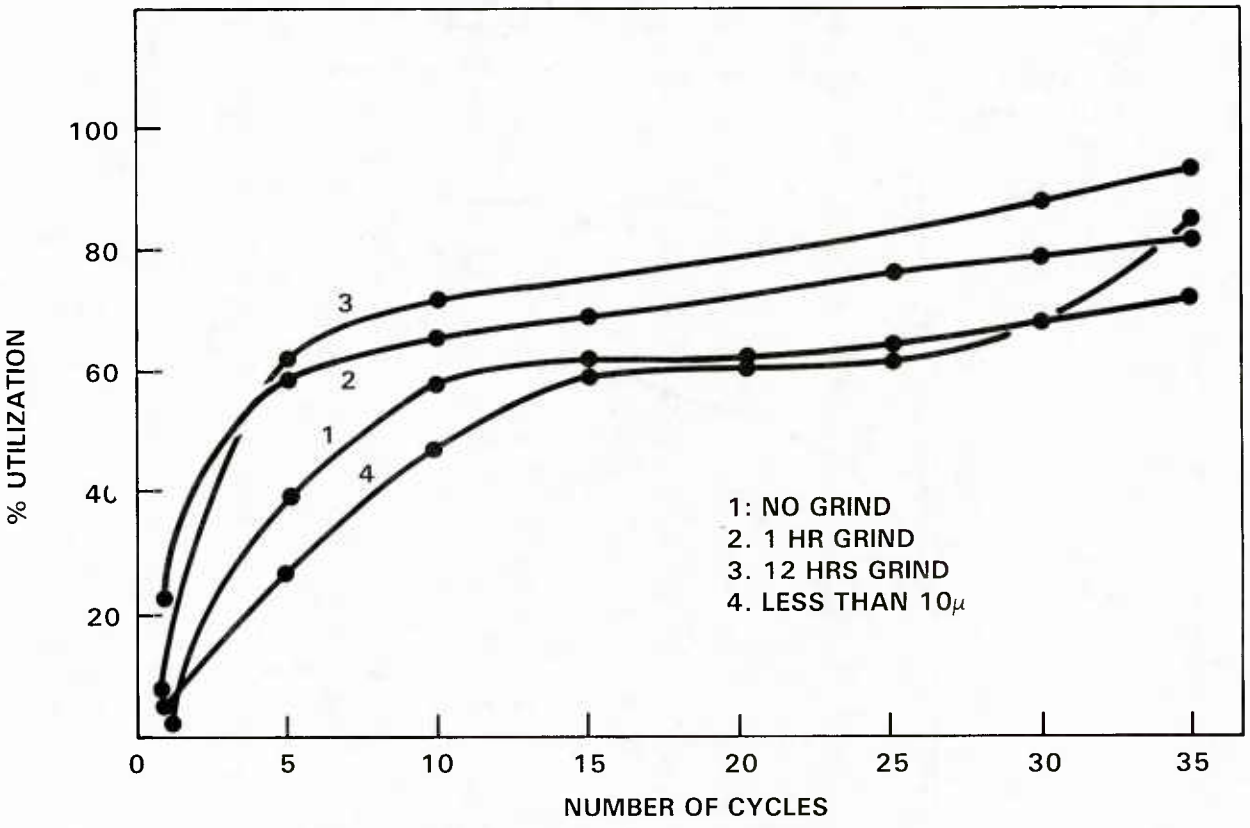

FIGURE 12. EFFECT OF ACTIVE MATERIAL PARTICLE SIZE ON UTILIZATION. (NICKEL HYDROXIDE PARTICLES ARE GROUND SUCCESSIVELY INTO SMALLER PARTICLES AND MIXED WITH COBALT HYDROXIDE UNIFORMLY BEFORE LOADING)

$Co(OH)_2$ particles uniformly before loading them into the composite plaques. There was a small improvement in the utilization with the reduction of particle size by grinding for 12 hours. However, when the particles were sifted through a 10 μm sieve after more than 12 hours of grinding, the charging efficiency decreased again. This is probably due to the difficulty associated with electrolyte penetration into the fine particle active material. Thus, reducing the particle size of the active material did not result in a quick utilization of the active material.

Surface Film of Additive on Active Material

The next attempt to achieve a quick, complete utilization of the active material was to treat the impregnated electrode with cobalt solution, although the active material in the electrode already contained some $Co(OH)_2$ additive. The surface treatment was made by either electrochemical or chemical method. In either method cobalt acetate solution was used to avoid possible contamination by NO_3^- or SO_4^{-2} ions.

The effect of the surface treatment is shown in Figure 13. When an electrode showing poor utilization was removed from the test cell and treated as above, in a cobalt solution (1.8 M), its utilization increased sharply. Other demonstrations of this effect of surface treatment are presented in Table 7 and Figures 14 and 15. Table 7 shows that the 30 mils (0.75 mm) thick composite electrode prepared by the electrochemical impregnation with surface treatment reached 96 percent utilization in the second cycle while the electrode that was prepared under the same conditions without the surface treatment exhibited a poor rise in utilization. Figure 14 shows the effect of the surface treatment and the manner of impregnation on the utilization. Electrodes represented by Figure 14-(a) are electrochemically impregnated and the electrodes represented by Figure 14-(b) are impregnated by the suspension method. In both cases, the effect of the surface treatment is quite dramatic. Although the effect is not as pronounced, electrodes fabricated by the suspension impregnation and surface treated also show a large improvement in utilization (Figure 14b). The effect of surface treatment in a thick plate (100 mils, 2.5 mm) is shown in Figure 15. There is a marked increase, but the increase in utilization with increasing number of cycles is not as steep as for a 30 mils plate. Either the surface treatment has not penetrated completely into the active material or there may be an inherent difficulty of electrolyte infiltration into the thick plate.

Electrodes under discussion to this point have been impregnated with solutions or mixtures containing a nominal 7 weight percent of cobalt compound. To determine whether bulk addition of cobalt compound to the active material is necessary for improvement in utilization, some electrodes were impregnated without the cobalt additive and subsequently surface treated with the Co solutions. The results of cycling test for these electrodes are presented in Figure 16. Figure 16 shows the effect of the duration of the surface treatment on the utilization. Using the Co surface treatment alone, the utilization behavior of these electrodes is comparable to those of the previous electrodes impregnated with the Co compound. There was some improvement between 10 and 20 seconds treatment time, however, a 120 seconds treatment did not provide any further improvement. $Co(OH)_2$ normally accounted for less than 3 percent of the $Ni(OH)_2$ active material on a weight basis. This demonstrates that the amount of additive can be reduced substantially (from 7 to 3 weight percent) by the surface treatment.

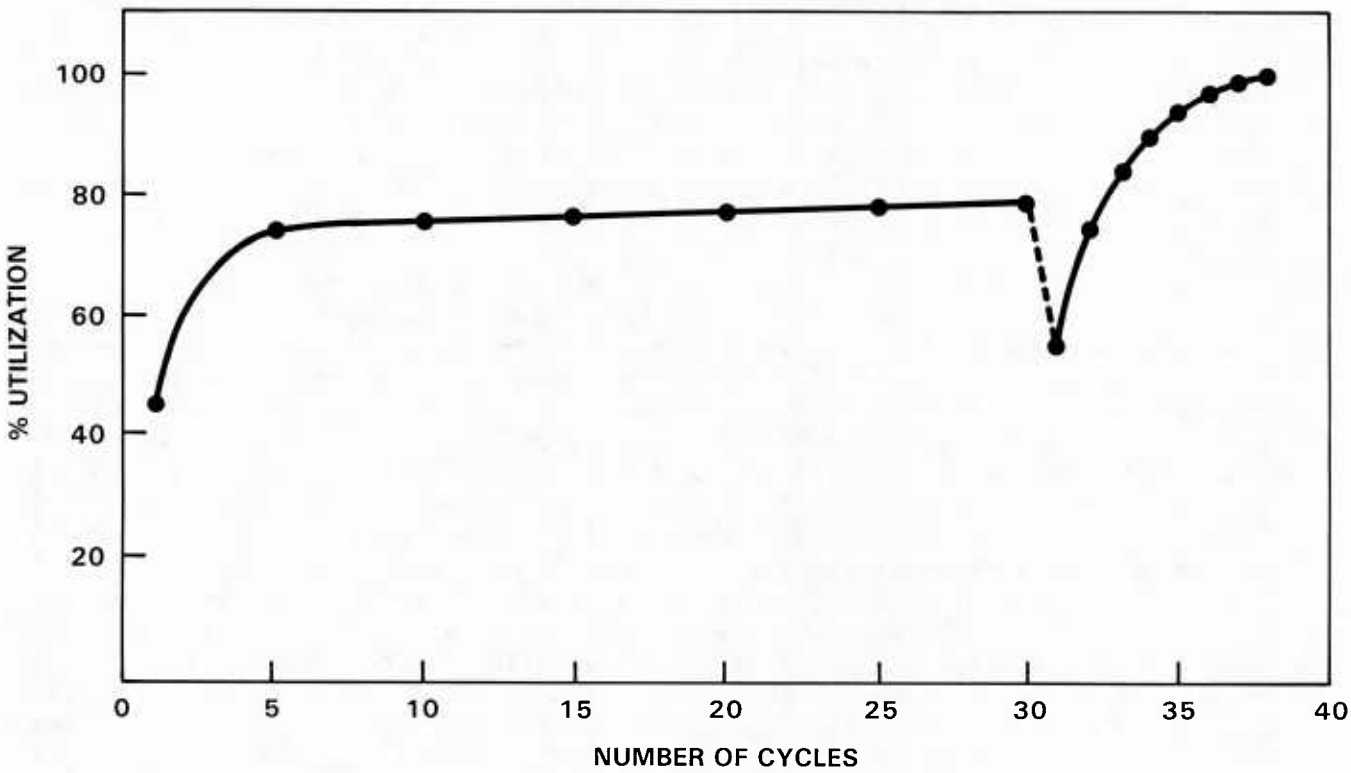

FIGURE 13. SUDDEN INCREASE OF THE UTILIZATION OF THE ACTIVE MATERIAL IN THE COMPOSITE PLAGUE (0.75mm THICK) AFTER THE SURFACE TREATMENT

TABLE 7. UTILIZATION OF ACTIVE MATERIAL IN COMPOSITE PLAQUE (IMPREGNATED IN 1.8M Ni^{2+} SOLUTION WITH 7% $Co(OH)_2$)

(a) Electrode Surface Treated with Co Solution.
Initial Plaque Weight: 0.790 gm,
Weight Gain After Impregnation: 0.979 gm,

Cycle No.	Utilization % 0.75V Cut-Off	1.0V Cut-Off
1	85	85
2	96	96
3	98	98
4	98	98
5	99	98
6	100	99

(b) Electrode with no Surface Treatment.
Initial Plaque Weight: 0.786 gm,
Weight Gain After Impregnation: 0.986 gm,

Cycle No.	Utilization % 0.75V Cut-Off	1.0V Cut-Off
1	56	56
2	65	65
3	68	68
4	70	70
5	72	72
6	72	72

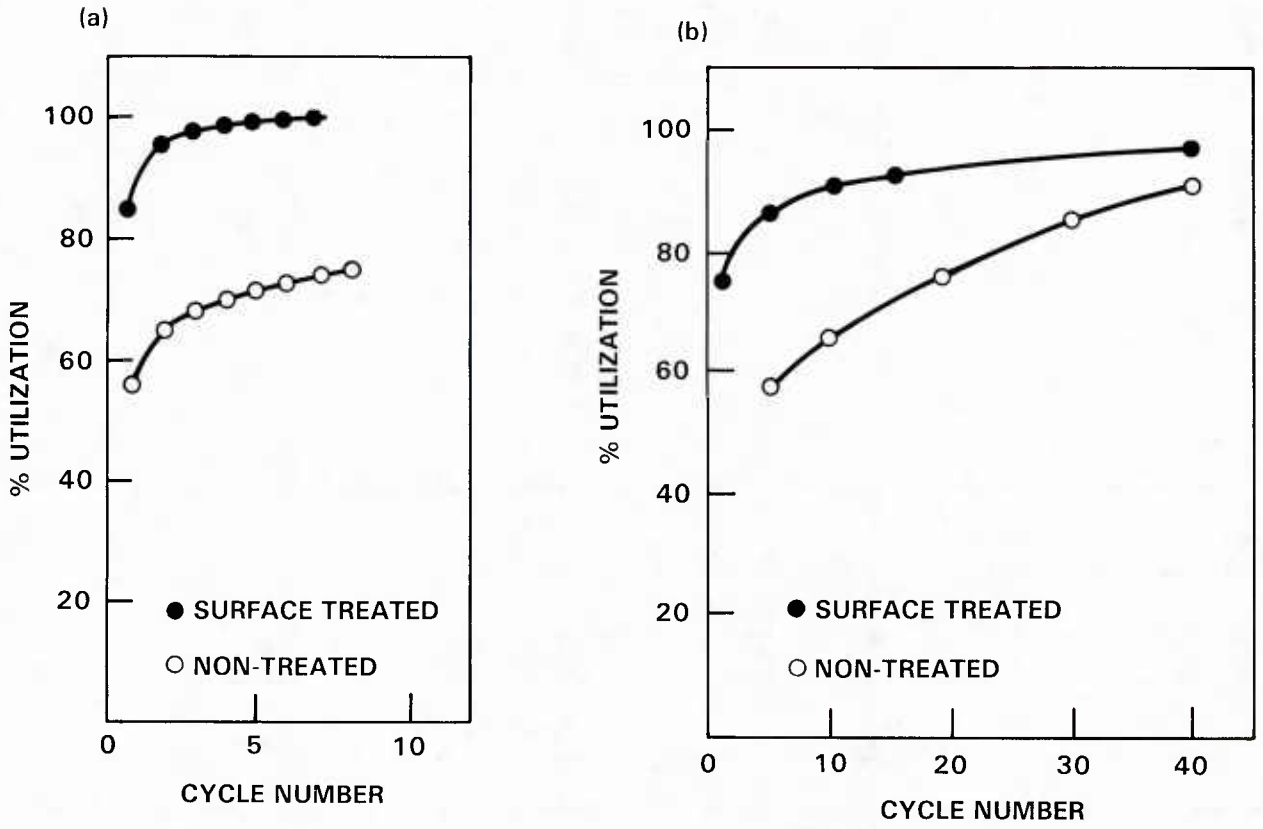

FIGURE 14. EFFECT OF THE SURFACE TREATMENT ON THE UTILIZATION RATE FOR COMPOSITE ELECTRODE (0.75mm THICK): IMPREGNATED BY (a) ELECTROCHEMICAL METHOD. (b) SUSPENSION METHOD

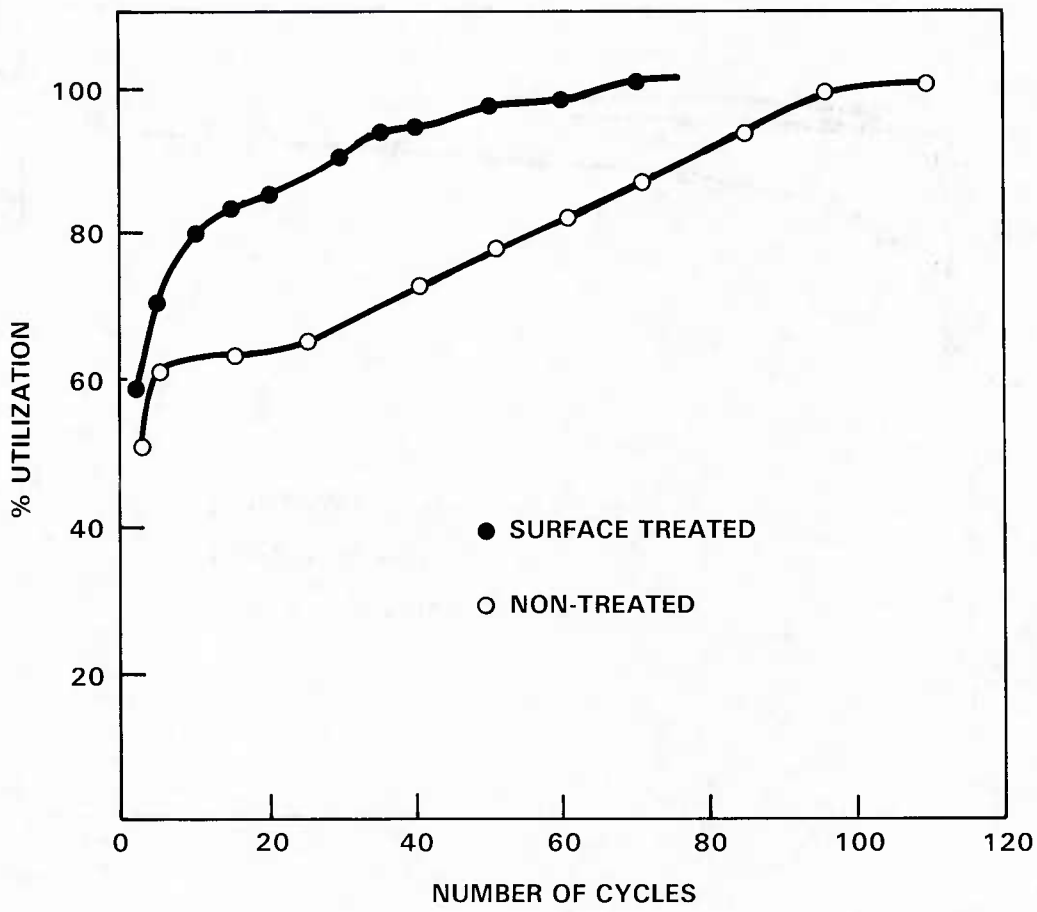

FIGURE 15. EFFECT OF THE SURFACE TREATMENT ON UTILIZATION OF THE 2.5mm THICK COMPOSITE ELECTRODE. (THE ELECTRODES ARE IMPREGNATED BY ELECTROCHEMICAL METHOD)

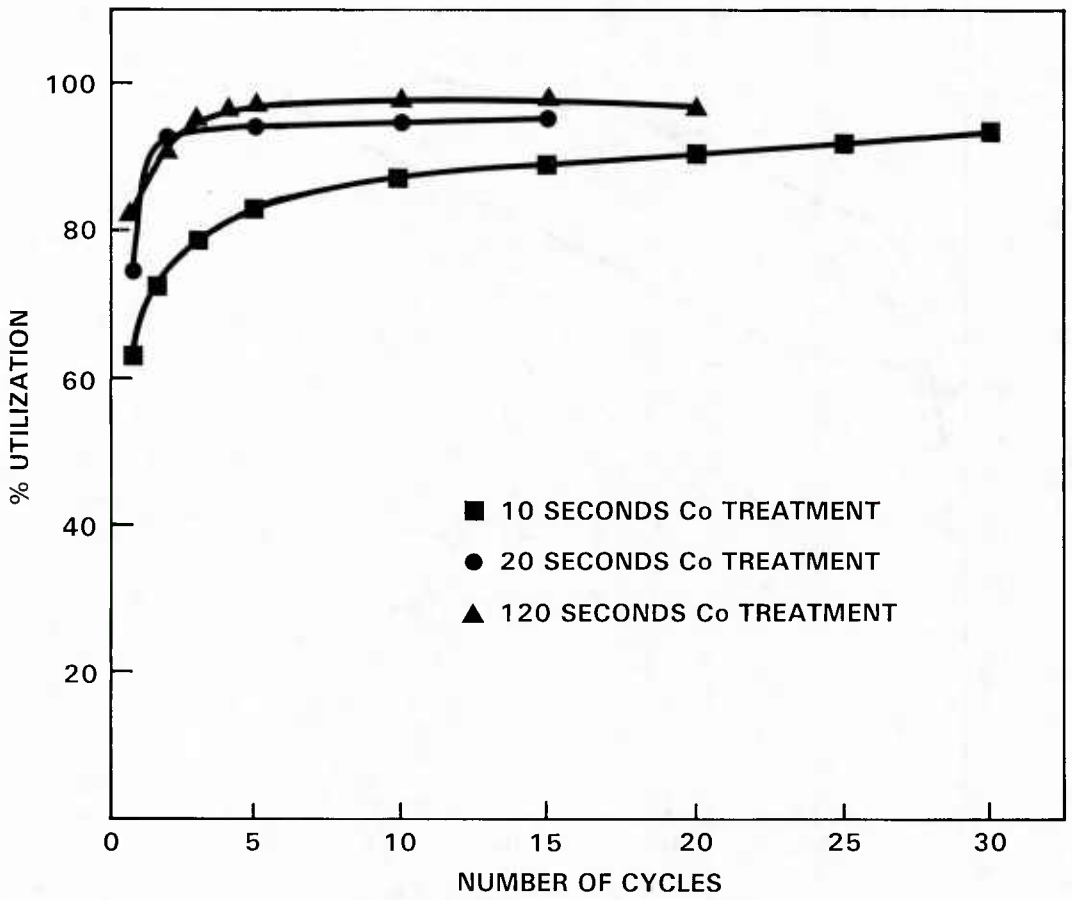

FIGURE 16. EFFECT OF THE DURATION OF SURFACE TREATMENT ON THE UTILIZATION OF THE ACTIVE MATERIAL WITHOUT $Co(OH)_2$ (.75mm THICK). (IMPREGNATED BY ELECTRO-CHEMICAL METHOD)

UTILIZATION VERSUS ADDITIVE DISTRIBUTION IN ACTIVE MATERIAL

These results have led to the development of a model to correlate the physical and chemical distribution of the active material with the utilization efficiency. Each type shown in Figure 11 is represented by a corresponding schematic distribution of both active material and additive inside the composite electrode (Figure 17).

The case of inhomogeneous additive distribution is pictured as type 2. $Co(OH)_2$ is heavily deposited in some local sites. The utilization varies from electrode to electrode depending on the distribution of the additive, but full utilization is seldom attained.

Type 3 shows the case in which a macroscopic homogeneity of additive is achieved, but on a small scale the additive still exists as a lump or is buried under the active material. These electrodes show a rather slow increase in utilization, but approach full utilization only after 50 or more cycles, Unlike the situation in type 2, $Co(OH)_2$ in this case eventually plays its role to enhance the activity of $Ni(OH)_2$ as the active material is rearranged during charge-discharge cycles. Electrodes prepared by suspension method show this type of behavior.

The morphology of active material in an electrode of ideal behavior is depicted by type 1 (Figure 17). In this electrode, the additive is not only uniformly distributed on a macroscopic scale but also covers the regions of active material, reachable by electrolyte ions, more thoroughly with its thin film layer. The surface layer additive on the active material can activate the material more effectively than when buried under it. The fact that the influence of an additive in $Ni(OH)_2$ is a surface effect was also demonstrated by Weininger[5] in his experiment using film electrodes. Another advantage of the surface treatment in activating nickel electrodes was shown by Winkler[6] in that the additive between $Ni(OH)_2$ particles can help maintain the primary structure of $Ni(OH)_2$. However, the quick rise of utilization by this type of treatment strongly suggests an electrocatalytic role of the additive at the initial phase of cycling in the charge-discharge reaction on the electrode surface.

In the case of powder sintered electrodes, the distinction between type 1 and 2 may be blurred because of their much smaller pore size. The exact location of $Co(OH)_2$ is not as critical in determining their utilization as the case of the composite body. Because of the large open pore structure of the composite plaques, the physical and chemical distribution of the active material in the plaques is far more sensitive to the impregnating conditions. Thus, depending on the impregnating conditions, the composite electrodes can exhibit any of the three different types of the behavior classified above.

Each type described thus far represents an extreme case. In many cases, the composite electrode could be better represented by a combination of these. The classification made above offers helpful guidance in understanding one aspect of the complicated behavior of the nickel composite electrode.

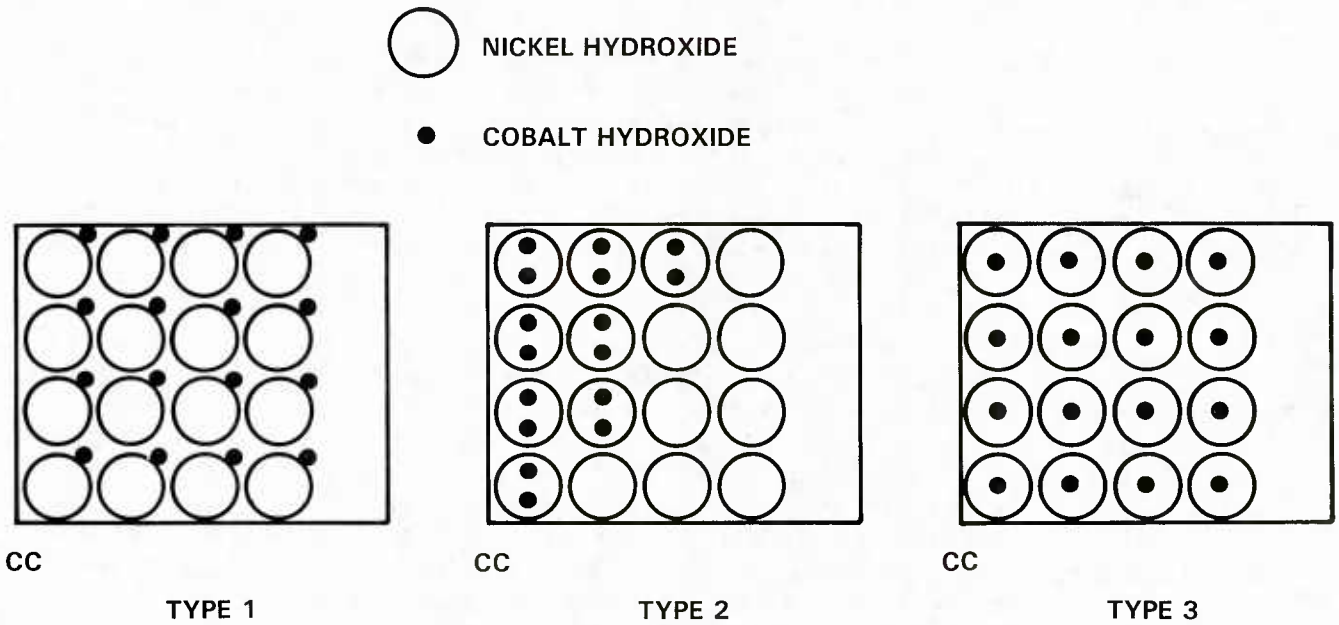

FIGURE 17. MODEL OF ACTIVE MATERIAL DISTRIBUTION IN THE NICKEL COMPOSITE ELECTRODE. (EACH MODEL REPRESENTS THE CORRESPONDING TYPE IN FIGURE 11. CC DENOTES CURRENT COLLECTOR)

CHAPTER 6

CONCLUSIONS AND RECOMMENDATIONS

CONCLUSIONS

Nickel composite plaques, despite a large open pore structure and irregular pore shape, can be impregnated efficiently electrochemically or chemically. The electrochemical process has been optimized for loading. About 60 percent higher current density (80 mA/cm^2) is required to impregnate the composite plaque in a 1.8M Ni^{2+} solution than the current density for sintered powder electrodes. By increasing Ni^{2+} concentration to 3.5M but using the same current density as for 1.8M Ni^{2+} solution, the impregnation time can be reduced to less than 1 hour (which is about one half of the time required for the impregnation in a 1.8M Ni^{2+} solution) to achieve the maximum loading level (1.6 gm/cc of plate volume). The impregnation time can be reduced further by increasing the current density, but at the cost of an increased risk of $Ni(OH)_2$ deposit on the outer surfaces of the composite plaques. Such a deposition can be suppressed by means of constant potential impregnation, lowering the bath temperature or employing intermittent current. Another advantage of the large open pore structure of the plaques is the ease of impregnating thick plaques (up to 2.5 mm thickness).

Probably one of the greatest advantages of the composite plaque over powder sinter is the possiblity of direct loading of externally prepared active material. This method achieves a loading level of the active material comparable with that by the electrochemical method, but in a much shorter time.

The manner of adding $Co(OH)_2$ additive was found to be critically important for a quick rise in utilization of $Ni(OH)_2$ active material in the sintered nickel composite body. By a proper surface treatment on the active material with the additive, the composite electrode can be activated to full utilization of its charge capacity in just five charge-discharge cycles.

This phenomenon reflects the unique pore structure of the sintered composite body that is not observed in the sintered powder body. It is proposed that the manner of adding the additive sensitively determines the pattern of its distribution throughout the active material in the composite body and accordingly dictates the utilization behavior of the composite electrodes.

RECOMMENDATIONS

The advancements made in impregnation techniques and surface treatment has solved most problems associated with the composite nickel electrode.

Future work should be concentrated on the optimization of the physical properties of the substrate such as: porosity, uniformity, fiber diameter and fiber nickel coating thickness. Another area for further investigation involves finding a more economical way to coat graphite fibers. A recently developed electrochemical plating technique (CYCOM, MCG Fiber Products, American Cynamid Corp., Wayne, NJ) already shows a substantial improvement both in cost and quality over the electroless coating method. A primary chemical deposition method - vapor plating directly with the $Ni(CO)_4$ - might yield further substantial cost reduction in nickel coating. Development of such a method, however, will require a rather intensive research effort and motivation from the prospect of relatively high volume product end use.

REFERENCES

1. Ferrando, W. A., Lee, W. W., and Sutula, R. A., "A Lightweight Nickel Composite Electrode I: Concept and Feasibility," Journal of Power Sources, Vol. 12, 1984, p. 249.

2. Ferrando, W. A., Lee, W. W., Lee, A. L., and Sutula, R. A., Physical Properties of the Nickel Composite Sintered Plaque, NSWC TR 82-416, Dec 1982.

3. Falk, S. U., and Salkind, A. J., Alkaline Storage Batteries (New York: John Wiley & Sons, Inc., 1969), pp. 48-52.

4. Hausler, E., "Electrochemical Impregnation of Porous Sintered Nickel Grids According to the Kandler-Process," in Power Sources 1966, Collins, D. H., Ed., (London: Pergamon Press, 1967), p. 287.

5. Weininger, J. L., "The Alkaline Nickel Hydroxide Electrode," Proceedings of the Symposium on the Nickel Electrode, Gunther, R. G., and Gross, S., Ed., Vol. 82-4, 1982, p. 1.

6. Winkler, H., "Improvements in or Relating to Process for Activating the Positive Electrodes of Alkaline Accumulators," British Patent No. 777,417, 1957.

7. Lee, A. L., Ferrando, W. A., and Flight, F. P., "Electrochemical Impregnation of Nickel Composite Electrodes," NSWC TR 82-414, Aug 1982.

8. Pickett, D. F., "Fabrication and Investigation of Nickel-Alkaline Cells, Part I: Fabrication of Nickel Hydroxide Electrodes Using Electrochemical Impregnation Techniques," AFAPL-TR-75-34, 1975.

9. Falk, S. U., and Salkind, A. J., Alkaline Storage Batteries, pp. 125-131.

10. Ferrando, W. A., and Lee, W. W., "A Suspension Method for Impregnating Sintered Nickel Composite Plaque," 31st Power Sources Symposium, Cherry Hill, NJ, Jun 1966.

11. Lee, W. W., Sutula, R. A., and Ferrando, W. A., "The Utilization of Nickel Hydroxide Active Material Impregnated in Graphite Composite Nickel Plaque," in Proceedings of Symposium on Porous Electrodes: Theory and Practice, Maru, H. C., et. al., Ed., Vol. 84-8, 1984, p. 32.

DISTRIBUTION

	Copies
Defense Technical Information Center Cameron Station Alexandria, VA 22314	12
Defense Nuclear Agency Attn: Library Washington, DC 20301	1
Pentagon Project Officer, OSD(MRA&L)-WR Attn: William G. Miller Room 2B323 Washington, DC 20301	1
Office of Deputy Under Secretary of Defense for Research and Engineering Staff Specialist for Materials and Structures Attn: Mr. Jerome Persh Room 3D1089, The Pentagon Washington, DC 20301	1
Defense Advanced Research Projects Agency Attn: E. Van Reuth L. Jacobsen 1400 Wilson Boulevard Arlington, VA 22209	1 1
Institute for Defense Analyses R&E Support Division 400 Army-Navy Drive Arlington, VA 22202	1
Library of Congress Attn: Gift and Exchange Division Washington, DC 20540	4
Office of Chief of Naval Operations Operation Evaluation Group Washington, DC 20350	1
David W. Taylor Naval Ship Research and Development Center Attn: A. B. Neild (Code 2723) W. J. Levendahl (Code 2703) J. Woerner (Code 2724) H. R. Urbach (Code 2724) D. Icenhower (Code 2721) J. Gudas (Code 2813) W. Lukens (Code 2822) Annapolis Laboratory Annapolis, MD 21402	1 1 1 1 1 1 1
Naval Air Development Center Attn: Dr. E. McQuillen Dr. G. London Warminster, PA 18974	1 1
Naval Air Systems Command Attn: Mr. R. Schmidt (Code 52031A) Washington, DC 20361	1
Naval Electronic Systems Command Attn: A. H. Sobel (Code PME 124-31) Washington, DC 20360	1
Naval Intelligence Support Center Attn: Dr. H. Ruskie (Code 362) 4301 Suitland Road Washington, DC 20390	1

DISTRIBUTION (Cont.)

	Copies
Naval Material Command	
Attn: Code 08T223	1
J. Kelly (MAT 0725)	1
W. Holden (MAT 08E4)	1
O. J. Remson (MAT 071)	1
G. R. Spaulding (MAT 072)	1
Washington, DC 20360	
Naval Ocean Systems Center	
Attn: Code 922	1
Dr. S. D. Yamomoto (Code 513)	1
P. D. Burke (Code 9322)	1
San Diego, CA 92152	
Naval Ordnance Station	
Attn: Howard R. Paul	1
Project Manager	
Southside Drive	
Louisville, KY 40150	
Naval Postgraduate School	
Attn: Dr. William M. Tolles (Code 612)	1
Monterey, CA 93940	
Naval Research Laboratory	
Attn: Dr. Fred Saalfeld (Code 6100)	1
A. Simon (Code 6130)	1
S. C. Sanday (Code 6370)	1
I. Wolock (Code 8433)	1
H. Chaskelis (Code 8431)	1
4555 Overlook Avenue, S.W.	
Washington, DC 20375	
Naval Sea Systems Command	
Attn: M. Kinna (Code 62R4)	1
J. DeCorpo	1
E. J. Anderson	1
Code 5433	1
H. Vanderveldt (Code 05R15)	1
Code 99612	2
Code 0841B	1
Washington, DC 20362	

	Copies
Naval Underwater Systems Center	
Attn: J. Moden (Code 36123)	1
R. Lazar (Code 36301)	1
Newport, RI 02841	
Naval Weapons Center	
Attn: A. Fletcher (Code 3852)	1
China Lake, CA 93555	
Naval Weapons Support Center	
Attn: M. Robertson	1
Electrochemical Power Sources Division	
Crane, IN 47522	
Office of Naval Research	
Attn: G. Neece (Code 413)	1
B. MacDonald (Code 471)	1
G. Sandoz (Code 715)	1
J. Smith (Code 413)	1
800 N. Quincy Street	
Arlington, VA 22217	
Strategic Systems Project Office	
Crystal Mall No. 3	
Attn: G. Needham (Code 273)	1
LCDR F. Ness (Code 234)	1
LCDR H. Nakayama (Code 272)	1
Washington, DC 20362	
Army Electronics Research and Development Command	
Attn: A. Legath (Code DELET-P)	2
S. Gilman (Code DRSEL-TL-P)	1
E. Brooks (Code DRSEL-TL-P)	1
G. DiMasi (Code DRSEL-TL-P)	1
Fort Monmouth, NJ 07703	
Army Foreign Science and Technology Center	
Attn: J. F. Crider (Code FSTC/DRXST-MTI)	1
220 7th Street	
Charlottesville, VA 22901	

DISTRIBUTION (Cont.)

	Copies
Army Materials & Mechanics Research Center	
Attn: J. J. DeMarco	1
J. N. McCauley	1
A. Levitt	1
J. Greenspan	1
F. Larson	1
L. R. Aronin	1
Watertown, MA 02172	
Army Material Development and Readiness Command	
Attn: J. W. Crellin (Code DRCDE-L)	1
5001 Eisenhower Avenue	
Alexandria, VA 22333	
Army Mobility Equipment R&D Command	
Attn: J. Sullivan (Code DRXFB)	1
G. D. Farmer, Jr. (Code DRDME-VM)	1
Dr. J. R. Huff (Code DRDME-EC)	1
Electrochemical Division	
Fort Belvoir, VA 22060	
Army Research Office	
Attn: B. F. Spielvogel	1
J. C. Hurt	1
P.O. Box 12211	
Research Triangle Park, NC 27709	
Army Scientific Liaison & Advisory Group	
Attn: HQDA (DAEN-ASR-SL)	1
Washington, DC 20314	
Ballistic Missile Defense Officer	
BMD-ATC	
Attn: M. L. Whitfield	1
P.O. Box 1500	
Huntsville, AL 35807	

	Copies
Office of Chief of Research & Development	
Attn: Dr. S. J. Magram	1
Department of the Army	
Energy Conversion Branch	
Room 410, Highland Building	
Washington, DC 20315	
Air Force Flight Dynamics Laboratory	
Attn: D. Roselius	1
L. Kelley	1
Wright-Patterson Air Force Base	
Dayton, OH 45433	
AF Weapons Laboratory	
Attn: Charles Stein	1
Kirtland AFB	
Albuquerque, NM 87115	
Air Force Wright Aeronautical Laboratory	
Attn: M. Duhl (Code MB)	1
T. Ronald (Code LLS)	1
W. S. Bishop (Code P00C-1)	1
R. M. Neff (Nonmetellic Mat. Div.)	1
D. R. Beeler (Code MB)	1
D. Marsh (Electrochemistry Code P00C-1)	1
Wright-Patterson AFB, OH 45433	
Frank J. Seiler Research Laboratory, AFSC	
Attn: LTCOL Lowell A. King (Code FJSRL/NC)	1
USAF Academy, CO 80840	
SD/YLXT	
Attn: MAJ R. Gajewski	1
P.O. Box 92960, WPC	
Los Angeles, CA 90009	

DISTRIBUTION (Cont.)

	Copies
Central Intelligence Agency	
Attn: C. Scuilla	1
G. Methlie	1
Washington, DC 20505	
Department of Energy	
Attn: Dr. A. Landgrebe (Code MS E-463)	1
Division of Applied Technology	
Washington, DC 20545	
Department of Energy	
Attn: L. J. Rogers (Code 2101)	1
Division of Electric Energy Systems	
Washington, DC 20545	
NASA Scientific and Technical Information Facility	
Attn: Library	1
P.O. Box 33	
College Park, MD 20740	
National Bureau of Standards	
Metallurgy Division	
Inorganic Materials Division	1
Washington, DC 20234	
NASA Lewis Research Center	
Attn: Mr. R. A. Signorelli	1
J. S. Fordyce (Code MS 309-1)	1
H. J. Schwartz (Code MS 309-1)	1
Cleveland, OH 44135	

	Copies
General Electric Company	
Re-entry Systems Operations	
Attn: K. J. Hall	1
P.O. Box 7722	
Philadelphia, PA 19101	
NASA Headquarters	
Attn: M. Greenfield (Code RTS-6)	1
Dr. J. H. Ambrus	1
600 Independence Avenue	
Washington, DC 20546	
NASA/Langley Research Center	
Attn: E. Mathauser (Code MS188A)	1
Dr. T. Bales	1
Dr. D. Tenney	1
Hampton, VA 23365	
Internal Distribution:	
E431	9
E432	3
R04 (P. Hesse)	1
R30 (J. R. Dixon)	1
R32 (R. A. Sutula)	1
R32 (W. A. Ferrando)	1
R32 (Staff)	5
R32 (W. W. Lee)	10
R33 (C. E. Mueller)	1
R301 (J. Hoff)	1
R35 (J. Hall)	1